THESIS

INTERACTION OF ERYTHROCYTES (RBC's) WITH NANOSTRUCTURED SURFACES

Submitted by

Harvinder Singh Virk

Department of Mechanical Engineering

In partial fulfillment of the requirements

For the Degree of Master of Science

Colorado State University

Fort Collins, Colorado

Summer 2022

Master's Committee:

Advisor: Ketul C. Popat

Soham Ghosh
Vivian Li

ABSTRACT

INTERACTION OF ERYTHROCYTES (RBC's) WITH NANOSTRUCTURED SURFACES

Titanium and its alloys are used to make different blood-contacting medical devices such as stents, artificial heart valves, and catheters for cardiovascular diseases due to their superior biocompatibility. Thrombus formation begins on the surface of these devices as soon as they encounter blood. This leads to the formation of blood clots, which obstructs the flow of blood that leads to severe complications. Recent advancements in nanoscale fabrication and superhydrophobic surface modification techniques have demonstrated that these surfaces have antiadhesive properties and the ability to reduce thrombosis. In this study, the interaction of erythrocytes and whole blood clotting kinetics on superhydrophobic titanium nanostructured surfaces was investigated. These surfaces were characterized for their wettability (contact angle), surface morphology and topography (scanning electron microscopy (SEM)), and crystallinity (glancing angled X-Ray diffraction (GAXRD)). Erythrocyte morphology on different surfaces was characterized using SEM and overall cell viability was demonstrated through fluorescence microscopy. The hemocompatibility of these surfaces was characterized using commercially available assays: thrombin generation assay → thrombin generation, hemolytic assay → hemolysis, and complement convertase assay → complement activity. The results indicate that superhydrophobic titanium nanostructured surfaces had lower erythrocyte adhesion, less morphological changes in adhered cells, lower thrombin generation, lower complement activation, and were less cytotoxic compared to control surfaces. Thus, superhydrophobic titanium

nanostructured surfaces may be a promising approach to prevent thrombosis for several blood-contacting medical devices.

Keywords: Hemocompatibility, titanium nanostructured surfaces, erythrocytes, thrombin generation, complement activation, hemolysis

ACKNOWLEDGEMENTS

First and foremost, I would like to thank my advisor, Dr. Ketul C. Popat, for his guidance from the beginning of my junior year up until now. I could not have asked for a more patient, caring, and intelligent mentor throughout my graduate work. He made time to answer all my questions even when he was busy. I think this wouldn't be possible without his help. Thank you.

I would like to thank Dr. Rebecca Miller from the chemistry department for teaching me how to operate a scanning electron microscope. This is the valuable skill I am sure will come in handy later in my career.

I would also like to thank Justin Gangwish of Colorado State University for his help in analyzing material samples for X-ray diffraction.

I would also like to thank Dr. Paolo Soares of Pontifical Catholic University of Paraná in Curitiba, Brazil for his help in analyzing material samples for X-ray spectroscopy.

I would also like to thank Iain Briongos of Colorado State University for his help in drawing blood for the experiments.

Finally, I would like to especially thank my colleagues in the lab: Dr. Robert Maia Sabino, Vignesh Manivasagam, and Prem Kantam. Roberta has always been so kind and helpful over the past three years. She has taught me almost every laboratory technique I know and has answered countless questions of mine. Vignesh had helped me a lot from taking SEM images to doing studies together. He taught me how to use different software that we used to analyze data. Prem was always wonderful to be around and have incredible work ethic. I wish you all the best in your future endeavors and I cannot wait to see what marvelous things you will accomplish.

DEDICATION

I would like to dedicate this thesis to my parents, uncle, and family. I think I wouldn't have come this far without their handwork and sacrifice. They are incredible and they supported me all through my career till date.

TABLE OF CONTENTS

LIST OF TABLES

LIST OF FIGURES

INTRODUCTION

Blood-contacting medical devices are commonly used in treating a wide variety of cardiovascular diseases. These devices are made from many different materials; however, titanium and its alloys have been widely used due to their favorable mechanical and chemical properties, and compatibility with many tissues in the body. Some examples of blood-contacting medical devices made from titanium and its alloys are stents, artificial heart valves, etc. [1]. However, titanium and its alloys are not hemocompatible and devices made from them are associated with the problems such as thrombosis. The imbalance of pro-and anti-coagulant factors in the blood that is in contact with the material surface results in thrombosis [2]. Previous studies have shown that the interaction of blood and its components with material surfaces is influenced by the surface properties, such as surface chemistry, morphology, and wettability [3], [4]. Blood clotting is initiated by protein adsorption. Fibrinogen is the predominant protein involved in this process and gets adsorbed on the surface immediately upon contact with blood [5]. The prothrombotic molecules are released due to the activation of fibrinogen [6]. After prothrombin is converted to thrombin, platelets adhere and activate on the surface. The mesh matrix is formed from the combination of fibrin and activated platelets. Erythrocytes get trapped in this mesh matrix. Thus, this initiates the erythrocytes adhesion and formation of blood clots [7]. These blood clots obstruct the flow of blood and can detach from the surface causing severe complications in different parts of the body. In certain cases, these devices can be replaced via revision surgery, however, these revision surgeries can be traumatic for the patients already suffering from cardiovascular disease. Thus, it is critical to design implant surfaces that are hemocompatible and prevent thrombosis in blood-contacting medical devices.

Previous studies have shown that the interaction of blood and its components with material surfaces can be controlled by changing surface properties such as topography, chemistry, and

wettability. The hemocompatibility of medical devices can be enhanced by modifying the surface using different techniques. These techniques result in reduced wettability of the surface resulting in lower protein adsorption, and lower platelet adhesion and activation on medical devices' surfaces eventually reducing blood clotting. The wettability is important because if the surface is hydrophilic, blood will disperse on the surface but there will be minimal to no contact when the surface is hydrophobic or superhydrophobic. Consequently, recent research has focused on improving hemocompatibility by modifying the surface topography of titanium. Studies have shown that altering the surface topography lowers the fibrinogen adsorption by 80% compared to the unmodified surface [8]. Altering the surface chemistry has shown a 12% and 67% decrease in platelet adhesion on superhemophobic titanium nanoflower and nanotubes surfaces, respectively, compared to unmodified surfaces [9]. This is because proteins binding with the surfaces are constrained by the strong binding of water molecules with the hydrophilic surface [5]. Studies have also shown that altering the wettability of the surface reduces the contact area between the liquid and the surface [8]. Minimal contact between blood and surface eventually will decrease blood clot formation. Thus, by modifying the surfaces, the interaction of proteins, platelets, and leukocytes can be controlled. However, not much research is done on the interaction of erythrocytes (RBCs) with the different surfaces. Since erythrocytes are an integral part of the process of thrombosis, it is important to evaluate their interaction with different surfaces. Inappropriate interaction of erythrocytes with surfaces may lead to their altered ability to carry enough oxygen to different parts of the body and result in further complications in patients.

In this study, nanostructured surfaces were fabricated from titanium, specifically using hydrothermal treatment and anodization. These nanostructured surfaces were also modified to be superhydrophobic. Erythrocytes were isolated from the whole human blood and incubated with different nanostructured surfaces. Titanium nanostructured surfaces were characterized using techniques as follows: surface wettability → contact angle goniometry, surface morphology → SEM, surface chemistry → XPS, surface crystallinity → XRD, and biocompatibility was assessed

using cytotoxicity → LDH assay, erythrocyte adhesion → fluorescence microscopy, erythrocyte morphology → SEM, thrombin generation → thrombin generation assay, hemolysis → hemolytic assay, and complement activity → complement convertase assay. hemolysis was evaluated to understand the effects of different surfaces on non-adhered cells. The thrombin generation on different surfaces was characterized because it is an important indicator of blood clot formation which requires erythrocytes. The complement activation was evaluated to analyze the biomaterial immune response. The results indicate that superhydrophobic nanostructured surfaces were not cytotoxic, prevented erythrocyte adhesion, prevented morphological changes in cells on the surface, and prevented thrombus formation. Thus, these surfaces have the potential of being used for different types of blood-contacting medical devices.

HYPOTHESIS AND SPECIFIC AIMS

Fundamental Hypothesis: Nanostructured surfaces can reduce the adhesion of erythrocytes.

Hypothesis 1: Titania **n**anostructured surfaces can be silanized to create stable superhydrophobic surfaces.

Specific Aim 1: Fabrication and modification of nanostructured surfaces. This specific aim is discussed in the chapter-2 and will cover:

a. Fabrication of uniformly distributed and reproducible titania nanoflower surfaces via hydrothermal synthesis.
b. Fabrication of uniformly distributed and reproducible titania nanotube surfaces via hydrothermal synthesis.
c. Fabrication of a superhydrophobic surface coating through modification of surface chemistry.
d. Characterization of titania nanostructured surfaces (surface chemistry, morphology, and crystallinity) and measurement of water contact angles.

Hypothesis 2: Superhydrophobic titania nanostructured surfaces can improve hemocompatibility and reduce erythrocyte adhesion.

Specific Aim 2: Evaluating erythrocytes' interaction with nanostructured surfaces. This specific aim is discussed in chapter-3 and will cover:

a. Investigation of surface cytotoxicity, cell morphology, and adhesion.
b. Investigation of hemolysis, thrombin generation, and complement activity.

CHAPTER 1

LITERATURE REVIEW

1.1 Introduction

Blood-contacting medical devices, such as stents, artificial heart valves, catheters, etc., are common and used in treating a wide variety of diseases. However, the imbalance of pro-and anti-coagulant factors in the blood caused by these devices results in thrombus formation (blood clots). The use of these devices gets complicated upon implantation due to thrombosis. Thrombosis occurs when the blood and its components treat medical devices as foreign objects. This triggers the thrombosis process by deposition and activation of blood components and the formation of blood clots. These clots can detach from the surface and cause severe complications. There are several approaches used to prevent thrombosis on implant surfaces. However, there are numerous drawbacks to these approaches. Hence, many researchers are actively researching to improve the bio-integration of blood-contacting medical devices. Generally, these approaches consist of treating medical devices with drugs or therapeutic coatings combined with the modification of surface topography, and chemistry. One of the most common approaches is prescribing patients with blood thinners such as aspirin, vorapaxar, and clopidogrel [10]. Another approach is coating implants with anticoagulants such as warfarin and heparin [11]. Presently, titanium and its alloys are widely used to make different types of medical devices due to their biocompatibility and favorable mechanical properties. In recent research, the surface of titanium is modified to form nanostructured surfaces. The focus is to modify the titanium dioxide (TiO_2) layer on the surface to improve surface hemocompatibility. The formed nanostructures from the titania layer resulted in improved compatibility with different cells present in the blood. Lately, the

surface chemistry of titania is modified to fabricate the superhydrophobic nanostructured surfaces. Results of these studies indicate reduced adhesion of blood components by inhibiting the interaction between surface and biological components. Therefore, superhydrophobic nanostructured surfaces show promise for reducing thrombosis on the surface but more data is needed to verify the potential of these fabricated surfaces.

1.2 Thrombus formation on surfaces

Healthy endothelial cells actively resist thrombosis in the arterial lining. On contrary, the artificial surface of implants promotes thrombosis through a series of complex interconnected processes [12]. Titanium and its alloys are not hemocompatible and devices made from them are associated with the problems such as thrombus formation. The imbalance of pro-and anti-coagulant factors in the blood in contact with titanium and its alloys results in thrombosis [2]. The immediate deposition of blood plasma proteins on the device surface initiates the thrombosis process. The body's immune system recognizes the implant as a foreign body that activates serine protease thrombin. Out of 300 distinct proteins, fibrinogen is the first protein to get adsorbed on the surface. It is converted to fibrin by the action of serine protease thrombin. Later, platelets and leukocytes adhered to the surface and get activated. Combined with fibrin, platelets, and leukocytes form a mesh-like structure in which erythrocytes get trapped and form thrombosis (blood clots) [12]. Glycoprotein complex IIb-IIIa mediates the adhesion of fibrinogen and platelets and can occur even when fibrinogen levels are extremely low [13], [14]. Different chemical indicators such as exposed collagen, thrombin [15] or negative surface charge can activate the adhered platelets [16]. Thromboxane A_2, adenosine phosphate (ADP), and other agonists are released by activated platelets which further mediates the process of adhesion, activation, and aggregation of more platelets [12]. The adhesion of leukocytes to the deposited fibrinogen occurs via complement receptor 3 of the complement activation system [17, p. 11], [18]. Beta-2 integrin Mac-1 gets activated when P-selectin adheres to the platelets and activates P-selectin

glycoprotein ligand-1 (PSGL-1) which is a counter receptor on leukocytes. This stabilizes the platelet-leukocyte aggregates [19]. The upregulation of leukocyte tissue factor, biosynthesis of several cytokines, and other inflammatory reactions are upregulated due to the interaction between P-selectin and PSGL-1 [19].

The formation of blood clots occurs when adsorbed fibrinogen is progressively replaced via the Vroman effect by proteins of the contact system. This includes factor (F) XII, high molecular weight kininogen, prekallikrein, and FXI [20]. FXIIa is part of an intrinsic pathway of coagulation cascade that initiates thrombin formation. This turns prekallikrein to kallikrein which activates more FXII [12, p.], [21]. The β-FXIIa is formed when kallikrein cleaves FXIIa. The classical pathway of the complement system is triggered due to the formation of β-FXIIa via activation of C1q complex protein [21], [22]. The two proteins C3 and C5 of the complement system are activated by kallikrein. C5 is activated by FIXa, FXa, and thrombin of the coagulation cascade [21]–[23]. Activated C3 and C5 further promote the adhesion and activation of leukocytes to artificial surfaces [22]. Thrombin generation and inflammatory response are increased due to the coagulation cascade and complement systems. Thrombin not only converts fibrinogen to fibrin but also serves as a platelet agonist and furthers platelet aggregation [12]. The polymerization of fibrin monomer on the surface stabilizes platelet aggregation which forms thrombus [12], [21]. Recent studies suggest that erythrocytes use chemical indicators to bind with fibrinogen, thrombin, and platelets [24], [25]. The exact mechanism and sequence of erythrocyte adhesion are unknown and research is carried out about their interaction with the surface of medical devices. The final form of thrombus matrix contains proteins, platelets, leukocytes, and erythrocytes. The formation of thrombus can cause device failure, obstruct the flow of blood, and these clots can cleave off causing severe complications in the patient's body. Therefore, it is necessary to develop medical devices which inhibit thrombosis, understanding the role and mechanisms of erythrocytes in thrombus formation.

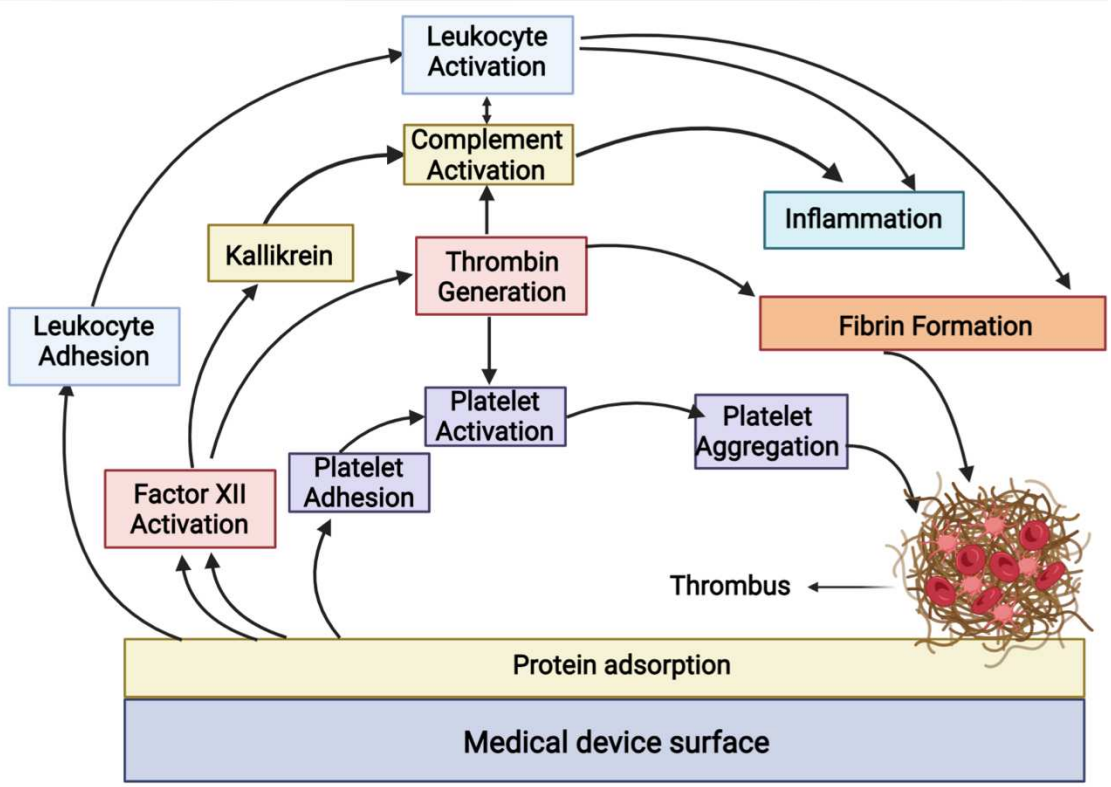

Figure 1.2.1: Graphical representation of thrombosis on medical device surfaces. Protein adsorption leads to platelet adhesion, activation, and aggregation. FXII absorbs and auto activates, converting prekallikrein to kallikrein while initiating coagulation and thrombin generation. Thrombin promotes platelet activation and converts fibrinogen into fibrin. Polymerized fibrin stabilizes platelet aggregates, forming a thrombus. Kallikrein, thrombin and other coagulation enzymes activate complement, inducing a local inflammatory response. Leukocytes are adhered, activated, and contribute to both coagulation and inflammation.

1.3 Blood-contacting devices

Cardiovascular Disease (CVD) remains the primary cause of global mortality, defying international efforts at prevention and outpacing all other forms of human disease despite its highly preventable, behavior-linked pathology. Data tracked by the American Heart Association and World Health Organization links over 31% of deaths internationally to CVD with the number of individuals afflicted with CVD within the United States projected to surpass 40% by 2030 [26]. CVD itself encompasses several associated pathologies attributed to the heart and blood vessels,

the most prominent being coronary artery disease (CAD) accounting for over 40% of all CVD-associated deaths [27]–[29]. Contemporary treatment techniques for CAD involve revascularization of the occluded vessel via percutaneous coronary intervention (PCI). Initial PCI methods solely relied upon balloon angioplasty to restore normalized flow through the afflicted vasculature but failed to maintain their therapeutic effect due to the prevalence of postoperative arterial recoil and coronary dissection, providing the momentum for the development of the modern coronary stent [30], [31]. In percutaneous coronary intervention procedures, roughly 90% of the time stents are used as they improve long-term patient outcomes. First, bare-metal stents (BMS) were constructed with metal alloys. There were different metals used for this such as stainless steel, cobalt, and nickel-titanium [30], [32]. The BMS are ideal due to their high mechanical strength which maintains the arterial diameter but scar tissue formation and thrombosis lead to restenosis [33]. To overcome these complications, drug-eluting stents (DES) were introduced and used in standard procedures. The DES stents were coated with heparin which releases sirolimus to the surrounding endothelium. This usually slows down the process of proliferation of vascular smooth muscle cells which contributes to stent restenosis [34]. The restenosis was greatly decreased by DES but the thrombosis occurs on the surface suddenly late after implantation as compared to BMS [33], [35]. After implantation, the thrombus formation is reduced by prescribing dual antiplatelet therapy (DAPT) with aspirin and clopidogrel, ticagrelor, or prasugrel for 6 to 12 months [21]. However, the drawbacks to this therapy are that it causes excessive bleeding and patients may become resistant to aspirin [36]. As a result, the fabrication of stents that can decrease both restenosis and thrombosis without any drawbacks became a priority.

The other form of blood-contacting medical device that's placed in patients is an artificial heart valve. Each year, more than 180,000 heart valve replacement surgeries are performed in the United States. Heart valves are either placed surgically or through a transcatheter procedure [37]. There are two types of heart valves that are used: Mechanical heart valves (MHVs) and

Biosynthetic heart valves (BHVs). The BHVs are fabricated from bovine or porcine tissue mounted on a metal frame [38]. The MHVs are more prone to thrombosis compared to BHVs. The lifespan of BHVs is about 10 to 20 years compared to MHVs which can last a patient's lifetime [39]. Thrombosis on the heart valve is not only increased through intrinsic pathways but also through hemodynamic and hemostatic factors. The turbulent flow is one of the factors of hemodynamics that can damage tissue around the protheses, initiate platelet adhesion, and prevent reendothelialization [38]. The congregation of coagulation factors near the tricuspid and mitral valve prostheses increase thrombosis compared to aortic valve prostheses [38]. The extrinsic pathway of the coagulation cascade is activated due to the tissue damage caused by the surgical insertion [38], [40]. Blood-thinning medications are prescribed to patients with MHVs to prevent thrombosis [41]. Generally, the hemocompatibility of blood-contacting devices must be improved to increase functionality and patients' health.

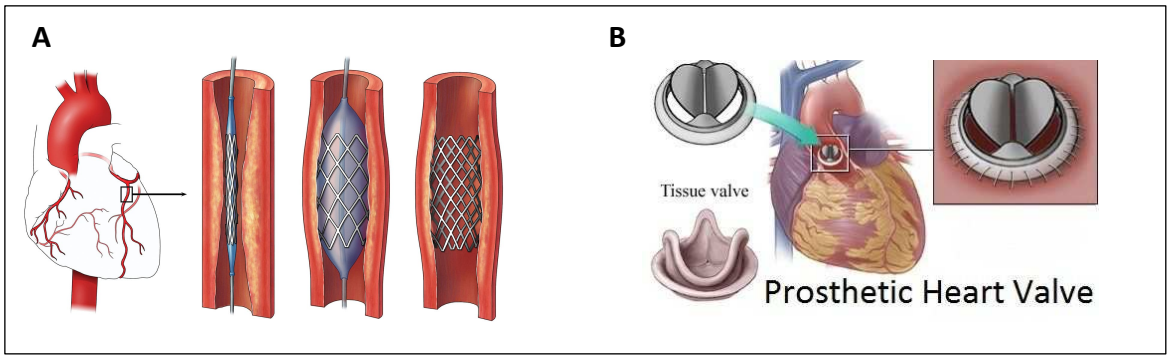

Figure 1.3.1: Some examples of blood-contacting medical devices: (A) Coronary Stent, and (B) mechanical heart valve. (A) adapted from Central Georgia Heart and Vein Center. "What do you need to know about a heart stent", (B) adapted from coherent market insights, "Prosthetic Heart Valve Market – Insights 2022".

1.4 Current solutions for thrombosis on biomedical devices

For prevention and treatment of thrombosis, antiplatelet agents are frequently used on blood-contacting devices. For example, after DES implantation DAPT is required which is combination of aspirin and a P2Y12 receptor inhibitor such as cyclooxygenase, prasugrel, or ticagrelor [42]. A set of enzymes that lead to the production of thromboxane A_2 which activate

platelets is inhibited using aspirin [43]. Aspirin is effective against thrombosis but it leads to internal bleeding in the gastrointestinal tract [36], [43], [44]. Due to prolonged use 40% of patients become drug resistant [44]. Drugs such as clopidogrel and prasugrel inhibits ADP-induced platelet aggregation by binding to the platelet receptor [43]. Ticagrelor is more effective than clopidogrel as it directly inhibits the platelet receptor but may increase risk of patient bleeding [45]. DAPT is more effective than aspirin treatment and recommended for 6-12 months to prevent thrombosis but research shows that it might be required beyond 1 year [46]. Anticoagulants such as heparin are also used in combination with antiplatelet therapies which blocks thrombin and FXa via antithrombin [21]. A drawback of heparin is that it induces thrombocytopenia which is non-reversible.

Modification to the surface of biomaterials seems to be a viable option to prevent thrombosis. Heparin coating is one of the prominent methods which is commercially available [2]. The drawback of heparin is their tendency to lose efficacy and generation of thrombocytopenia (HIT). In HIT, there are risks associated with a decrease in platelet count, body pain, and internal bleeding which leads to increase risk of thrombosis [47]. Polyethylene glycol (PEG) coatings, albumin coatings, and endothelial cell coatings are some other methods that are used to prevent thrombosis. In endothelial cell coatings, the reendothelialization is attempted on the devices by seeding the surfaces with endothelial cells [48]. There are problems related to these solutions such as inefficacy in vivo models, and difficulty in finding an effective scaffold. Nitric oxide (NO) is a naturally occurring which is currently being investigated for its antithrombic effects. The NO is used to maintain and construct the healthy blood vessels [49]. The NO works in vitro conditions but has not been tested in vivo conditions [49]. There is a need of a biocompatible surface which can decrease the effect of thrombosis. Superhydrophobic nanostructured surfaces does not adhere the blood components and therefore a promising surface modification explored in recent research.

1.5 Superhydrophobic materials

The biomimicry of superhydrophobic surfaces in nature such as lotus led to the development of superhydrophobic surfaces for different engineering applications [50]–[54]. There are three different categories in which surfaces are divided based on their wettability (interaction with liquids): hydrophilic if θ < 90°, hydrophobic if θ > 90°, and superhydrophobic if θ > 150°. The surface texture and energy play a vital role to make the surface superhydrophobic. The different effects can be explained through theoretical framework: Young, Wenzel, and Cassie-Baxter states [55]–[57]. In general, the contact angle (θ) on a surface droplet is related to the surface tension of its solid, liquid, and vapor interfaces using Young's equation [57]:

$$\cos\theta = \frac{\gamma_{SV}-\gamma_{SL}}{\gamma_{SL}} \quad \textbf{(1-1)}$$

where γ is surface energy per unit surface area of the interfaces of solid (S), liquid (L), and vapor (V) phases. Nonetheless, Young's equation does not account for surface roughness. In 1936, Wenzel modified the Young's equation which incorporated the surface roughness parameter [56], [58]:

$$\cos\theta_W = r\cos\theta \quad \textbf{(1-2)}$$

where θ_W is the apparent contact angle in the Wenzel state and r is the ratio of actual surface area to projected surface area (r=1 for a smooth surface and r>1 for a rough surface). The solid-liquid interfacial area is increased in the Wenzel state due to the permeation of liquid into the surface topography [59]. Cassie-Baxter state is a metastable state in which the air pockets are created between the liquid and surface topography, thus minimizing the interaction, and leading to a high apparent contact angle [51]:

$$\cos\theta_{CB} = f(1 + \cos\theta) - 1 \quad \textbf{(1-3)}$$

where θ_{CB} is the apparent contact angle in the Cassie-Baxter state and f is the ratio of solid-liquid area to solid-liquid and liquid-air area at the solid-liquid interface. A depiction of all three wetting categories is shown below (**Figure 1.5.1**).

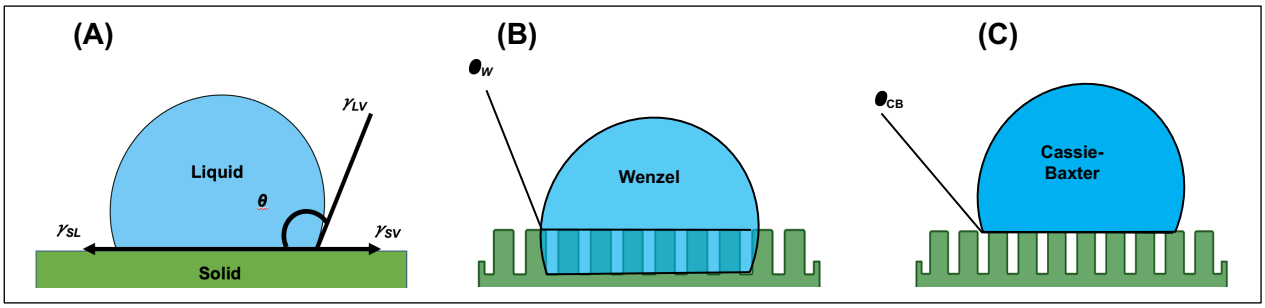

Figure 1.5.1: Depiction of (A) Young, (B) Wenzel, and (C) Cassie-Baxter wetting states.

The fabrication of superhydrophobic surfaces can be achieved via different techniques which includes chemical and physical methods. In this process, either the surface-energy of the surface was lowered or a low surface energy surface was used. Roughening was done using low surface-energy surfaces like fluorinated and perfluorinated silanes, phosphates, monomers, polymers, and copolymers because they contain low surface-energy functional groups (e.g. $-CF_2$, $-CF_2H$, $-CF_3$, etc.) [60], [61]. Methods to fabricate rough surfaces that allow superhydrophobicity are varied. Straightforward and effective methods such as etching with plasma, laser, and chemical are used to fabricate rough surfaces [61]. Other methods such as lithography is also widely used to roughen the surfaces which includes optical, nanoimprints, X-ray etc. [55]. Different techniques such as anodization, sol-gel processing, layer-by-layer self-assembly, electrospinning, and hydrothermal synthesis processes are also used to fabricate rough surfaces [61], [62].

When the surface energy of the rough surfaces is lowered the surfaces becomes superhydrophobic. The surface energy of the surfaces is changed using silane compounds via

silanization process. The properties such as adsorption and hydrophilicity/hydrophobicity are modified using silanes. There are different organofunctional groups present in the silane compounds such as linkage CH_2 groups, a silicone (Si) atom, and three hydrolysable groups [63]. In case of superhydrophobic surfaces, functional groups such as fluorine groups (-CF_2, and -CF_3) lowers the surface energy. The molecular mobility can be controlled by customizing the distance of functional groups from the surface. The silicone atom of silane covalently binds to the hydroxyl groups present on the surface to form a thin layer of silane. The polar surface interactions with water is shielded by the non-polar interphase and attached functional groups (**Figure 1.5.2**) [64].

The antiadhesive properties of superhydrophobic surfaces allows in to be used in numerous applications such as anti-icing [65], drag reduction [66], self-cleaning surfaces [67], oil and water separation [68] etc. Recent research on superhydrophobic surfaces shows a potential usage in blood-contacting medical devices. In thrombosis, the deposition of blood plasma proteins is the first step that initiates the process. The platelet adhesion can be reduced if the proteins such as fibrinogen does not get adsorbed to the surface. Previous studies have shown reduced platelet adhesion on superhydrophobic surfaces [9], [69]–[71]. This leads to reduction in initial thrombosis and improved overall hemocompatibility. More research is needed to understand the interaction of superhydrophobic surfaces with blood components, especially with erythrocytes. Titanium can form superhydrophobic surface coatings and may serve as a promising biocompatible substrate.

1.6 Titanium and titania nanomodification in biomaterials

Titanium and its alloys are widely used as biomedical implants due to their biocompatibility, mechanical properties, and high corrosion resistance [72]. More than 50 years, titanium and its alloys have been extensively used in dental and orthopedic implants [72]. They

are also used to make artificial heart valves and coronary stents [72]. The titanium surface is protected due to the formation of titanium dioxide when titanium reacts with oxygen. Numerous research has been conducted by forming different nanostructured surface from titanium such as nanowires, nanopores, nanoleaves, nanoflowers, etc. Same surface roughness techniques are used to fabricate nanostructures on titanium. The common techniques to form nanostructures on the surface are: Hydrothermal synthesis for NF and electrochemical anodization for NT. Titanium is etched by HF in both cases to form NF and NT, respectively. TiO_2 is formed into petals under hydrothermal conditions. Vertically aligned TiO_2 nanotube arrays are formed in electrochemical anodization. The formation of these nanoscale features on the surface which mimics the real bone tissue shows improved osteoblast proliferation and adhesion [73]. When compared to unmodified titanium, nanotubes have shown decreased immune response after 7-day incubation in whole blood [74]. The nanostructured surfaces have been modified with numerous bioactive components and shown improved hemocompatibility [75].

Nanostructures have shown biocompatibility in several different cellular tissues. The rough topography and cellular compatibility make nanostructures an ideal surface for forming superhydrophobic surfaces. The results from interaction of blood components with superhydrophobic surfaces indicate decrease in cell adhesion and improve hemocompatibility compared to control titanium [8], [69]. In a recent study, less platelet adhesion and activation was observed on superhydrophobic nanoflowers compared to control titanium [70]. However, all other thrombosis releated processes were investigated, except erythrocytes adhesion. The hemocompatibility of the nanostructured surfaces have not been characterized. There is no known study in the literature where interaction of superhydrophobic nanostructures was extensively observed. Therefore, for the first time, this work seeks to explain the hemocompatibility of the superhydrophobic nanostructured surfaces and erythrocyte adhesion on these surfaces.

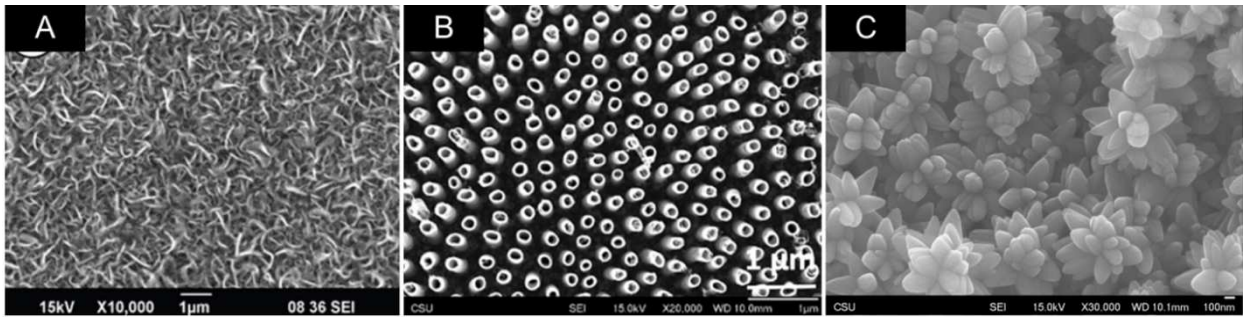

Figure 1.6.1: Examples of titania (A) nanoleaves, (B), nanotubes, and (C) nanoflowers. (B) and (C). (A) adapted with permission from John Wiley and Sons: [Advanced Healthcare Materials Vol. 6 Iss. 11] C.C. Mohan, A.M. Cherian, S. Kurup, J. Joseph, M.B. Nair, M. Vijayakumar, S. V. Nair, D. Menon, Stable Titania Nanostructures on Stainless Steel Coronary Stent Surface for Enhanced Corrosion Resistance and Endothelialization. Copyright (2017). [117]. (B) adapted with permission from The Royal Society of Chemistry: [RSC Advances Vol. 7] K. Bartlet, S. Movafaghi, A. Kota, K.C. Popat, Superhemophobic titania nanotube array surfaces for blood contacting medical devices. Copyright (2017). License at https://creativecommons.org/licenses/by-nc-sa/3.0/ [99].

REFERENCES

[1] I. H. Jaffer and J. I. Weitz, “The blood compatibility challenge. Part 1: Blood-contacting medical devices: The scope of the problem,” *Acta Biomater.*, vol. 94, pp. 2–10, Aug. 2019, doi: 10.1016/j.actbio.2019.06.021.

[2] M. F. Maitz *et al.*, “The blood compatibility challenge. Part 4: Surface modification for hemocompatible materials: Passive and active approaches to guide blood-material interactions,” *Acta Biomater.*, vol. 94, pp. 33–43, Aug. 2019, doi: 10.1016/j.actbio.2019.06.019.

[3] M. F, B. C, T. L, and R. K, “Controlling protein-particle adsorption by surface tailoring colloidal alumina particles with sulfonate groups.,” *Acta Biomater.*, vol. 9, no. 3, pp. 5780–5787, Nov. 2012, doi: 10.1016/j.actbio.2012.11.012.

[4] H. Fabre, D. Mercier, A. Galtayries, D. Portet, N. Delorme, and J.-F. Bardeau, “Impact of hydrophilic and hydrophobic functionalization of flat TiO2/Ti surfaces on proteins adsorption,” *Appl. Surf. Sci.*, vol. 432, pp. 15–21, Feb. 2018, doi: 10.1016/j.apsusc.2017.08.138.

[5] L.-C. Xu, J. Bauer, and C. A. Siedlecki, “Proteins, Platelets, and Blood Coagulation at Biomaterial Interfaces,” *Colloids Surf. B Biointerfaces*, vol. 124, pp. 49–68, Dec. 2014, doi: 10.1016/j.colsurfb.2014.09.040.

[6] “Thrombus Formation - an overview | ScienceDirect Topics.” https://www.sciencedirect.com/topics/engineering/thrombus-formation (accessed Jun. 07, 2022).

[7] L. A. Wells, H. Guo, A. Emili, and M. V. Sefton, “The profile of adsorbed plasma and serum proteins on methacrylic acid copolymer beads: Effect on complement activation,” *Biomaterials*, vol. 118, pp. 74–83, Feb. 2017, doi: 10.1016/j.biomaterials.2016.11.036.

[8] R. M. Sabino, K. Kauk, S. Movafaghi, A. Kota, and K. C. Popat, “Interaction of Blood Plasma Proteins with Superhemophobic Titania Nanotube Surfaces,” *Nanomedicine Nanotechnol. Biol. Med.*, vol. 21, p. 102046, Oct. 2019, doi: 10.1016/j.nano.2019.102046.

[9] S. Movafaghi *et al.*, “Hemocompatibility of Superhemophobic Titania Surfaces,” *Adv. Healthc. Mater.*, vol. 6, no. 4, p. 1600717, 2017, doi: 10.1002/adhm.201600717.

[10] H. Jneid, D. L. Bhatt, R. Corti, J. J. Badimon, V. Fuster, and G. S. Francis, “Aspirin and clopidogrel in acute coronary syndromes: therapeutic insights from the CURE study,” *Arch. Intern. Med.*, vol. 163, no. 10, pp. 1145–1153, May 2003, doi: 10.1001/archinte.163.10.1145.

[11] H. Wang *et al.*, “Heparin free coating on PLA membranes for enhanced hemocompatibility via iCVD,” *Appl. Surf. Sci.*, vol. 433, pp. 869–878, Mar. 2018, doi: 10.1016/j.apsusc.2017.10.123.

[12] I. H. Jaffer, J. C. Fredenburgh, J. Hirsh, and J. I. Weitz, “Medical device-induced thrombosis: what causes it and how can we prevent it?,” *J. Thromb. Haemost. JTH*, vol. 13 Suppl 1, pp. S72-81, Jun. 2015, doi: 10.1111/jth.12961.

[13] B. Savage and Z. M. Ruggeri, “Selective recognition of adhesive sites in surface-bound fibrinogen by glycoprotein IIb-IIIa on nonactivated platelets,” *J. Biol. Chem.*, vol. 266, no. 17, pp. 11227–11233, Jun. 1991.

[14] W. B. Tsai, J. M. Grunkemeier, and T. A. Horbett, “Human plasma fibrinogen adsorption and platelet adhesion to polystyrene,” *J. Biomed. Mater. Res.*, vol. 44, no. 2, pp. 130–139, Feb. 1999, doi: 10.1002/(sici)1097-4636(199902)44:2<130::aid-jbm2>3.0.co;2-9.

[15] “Platelet Activation: The Mechanisms and Potential Biomarkers.” https://www.hindawi.com/journals/bmri/2016/9060143/ (accessed Jun. 27, 2022).

[16] L. Tremolizzo, G. Sala, and C. Ferrarese, “Platelet Activation,” in *Encyclopedia of Psychopharmacology*, I. P. Stolerman, Ed. Berlin, Heidelberg: Springer, 2010, pp. 1034–1035. doi: 10.1007/978-3-540-68706-1_808.

[17] J. D. Loike *et al.*, “CD11c/CD18 on neutrophils recognizes a domain at the N terminus of the A alpha chain of fibrinogen.,” *Proc. Natl. Acad. Sci.*, vol. 88, no. 3, pp. 1044–1048, Feb. 1991, doi: 10.1073/pnas.88.3.1044.

[18] S. D. Wright, J. I. Weitz, A. J. Huang, S. M. Levin, S. C. Silverstein, and J. D. Loike, “Complement receptor type three (CD11b/CD18) of human polymorphonuclear leukocytes recognizes fibrinogen.,” *Proc. Natl. Acad. Sci.*, vol. 85, no. 20, pp. 7734–7738, Oct. 1988, doi: 10.1073/pnas.85.20.7734.

[19] C. Cerletti, C. Tamburrelli, B. Izzi, F. Gianfagna, and G. de Gaetano, “Platelet-leukocyte interactions in thrombosis,” *Thromb. Res.*, vol. 129, no. 3, pp. 263–266, Mar. 2012, doi: 10.1016/j.thromres.2011.10.010.

[20] P. Turbill, T. Beugeling, and A. A. Poot, “Proteins involved in the Vroman effect during exposure of human blood plasma to glass and polyethylene,” *Biomaterials*, vol. 17, no. 13, pp. 1279–1287, Jul. 1996, doi: 10.1016/S0142-9612(96)80004-4.

[21] M. Gorbet, C. Sperling, M. F. Maitz, C. A. Siedlecki, C. Werner, and M. Sefton, “The Blood Compatibility Challenge.” Rochester, NY, Mar. 01, 2019. doi: 10.2139/ssrn.3345274.

[22] “Interaction Between the Coagulation and Complement System | SpringerLink.” https://link.springer.com/chapter/10.1007/978-0-387-78952-1_6 (accessed Jun. 27, 2022).

[23] M. J. Krisinger *et al.*, “Thrombin generates previously unidentified C5 products that support the terminal complement activation pathway,” *Blood*, vol. 120, no. 8, pp. 1717–1725, Aug. 2012, doi: 10.1182/blood-2012-02-412080.

[24] R. I. Litvinov and J. W. Weisel, “Role of red blood cells in haemostasis and thrombosis,” *ISBT Sci. Ser.*, vol. 12, no. 1, pp. 176–183, 2017, doi: 10.1111/voxs.12331.

[25] J. R. Byrnes and A. S. Wolberg, “Red blood cells in thrombosis,” *Blood*, vol. 130, no. 16, pp. 1795–1799, Oct. 2017, doi: 10.1182/blood-2017-03-745349.

[26] “Heart Disease and Stroke Statistics—2017 Update: A Report From the American Heart Association | Circulation.” https://www.ahajournals.org/doi/10.1161/cir.0000000000000485 (accessed Oct. 05, 2020).

[27] J. Stewart, G. Manmathan, and P. Wilkinson, “Primary prevention of cardiovascular disease: A review of contemporary guidance and literature,” *JRSM Cardiovasc. Dis.*, vol. 6, p. 2048004016687211, Dec. 2017, doi: 10.1177/2048004016687211.

[28] “Cardiovascular diseases (CVDs).” https://www.who.int/news-room/fact-sheets/detail/cardiovascular-diseases-(cvds) (accessed Oct. 05, 2020).

[29] CDC, “Heart Disease Facts | cdc.gov,” *Centers for Disease Control and Prevention*, Sep. 08, 2020. https://www.cdc.gov/heartdisease/facts.htm (accessed Oct. 05, 2020).

[30] J. Iqbal, J. Gunn, and P. W. Serruys, “Coronary stents: historical development, current status and future directions,” *Br. Med. Bull.*, vol. 106, pp. 193–211, 2013, doi: 10.1093/bmb/ldt009.

[31] S. Borhani, S. Hassanajili, S. H. Ahmadi Tafti, and S. Rabbani, “Cardiovascular stents: overview, evolution, and next generation,” *Prog. Biomater.*, vol. 7, no. 3, pp. 175–205, Sep. 2018, doi: 10.1007/s40204-018-0097-y.

[32] D. He, W. Liu, and T. Zhang, “The Development of Carotid Stent Material,” *Interv. Neurol.*, vol. 3, no. 2, pp. 67–77, 2014, doi: 10.1159/000369480.

[33] “Coronary Stents: Current Status - ScienceDirect.” https://www.sciencedirect.com/science/article/pii/S0735109710023715?via%3Dihub (accessed Jun. 27, 2022).

[34] “Subacute stent thrombosis associated with a heparin-coated stent and heparin-induced thrombocytopenia - Cruz - 2003 - Catheterization and Cardiovascular Interventions - Wiley Online Library.” https://onlinelibrary.wiley.com/doi/full/10.1002/ccd.10366?casa_token=LH6a5ZMQDd0AAAA%3AG5M7wHAnJJ6vbExYVaByv8lMfUzxuLsQdWRNvL4CpGUhMwHrZ-5A5IPMfkUw7cfasho9cu-2dR8OHigq (accessed Jun. 27, 2022).

[35] D. R. Holmes *et al.*, “Stent Thrombosis,” *J. Am. Coll. Cardiol.*, vol. 56, no. 17, pp. 1357–1365, Oct. 2010, doi: 10.1016/j.jacc.2010.07.016.

[36] “Aspirin resistance - The Lancet.” https://www.thelancet.com/journals/lancet/article/PIIS0140-6736(06)68040-9/fulltext (accessed Jun. 27, 2022).

[37] L. J. Davidson and C. J. Davidson, “Transcatheter Treatment of Valvular Heart Disease: A Review,” *JAMA*, vol. 325, no. 24, pp. 2480–2494, Jun. 2021, doi: 10.1001/jama.2021.2133.

[38] G. D. Dangas, J. I. Weitz, G. Giustino, R. Makkar, and R. Mehran, “Prosthetic Heart Valve Thrombosis,” *J. Am. Coll. Cardiol.*, vol. 68, no. 24, pp. 2670–2689, Dec. 2016, doi: 10.1016/j.jacc.2016.09.958.

[39] “2020 ACC/AHA Guideline for the Management of Patients With Valvular Heart Disease: A Report of the American College of Cardiology/American Heart Association Joint Committee on Clinical Practice Guidelines | Circulation.” https://www.ahajournals.org/doi/10.1161/CIR.0000000000000923 (accessed Jun. 27, 2022).

[40] J. Luszczak, A. Undas, M. Gissel, M. Olszowska, and S. Butenas, “Activated factor XI and tissue factor in aortic stenosis: Links with thrombin generation,” *Blood Coagul. Fibrinolysis Int. J. Haemost. Thromb.*, vol. 22, no. 6, pp. 473–479, Sep. 2011, doi: 10.1097/MBC.0b013e328346c2bb.

[41] T. Owais *et al.*, “Anticoagulation After Biological Aortic Valve Replacement: Is There An Optimal Regimen?,” *J. Heart Valve Dis.*, vol. 25, no. 2, pp. 139–144, Mar. 2016.

[42] “Dual Antiplatelet Therapy After Drug-eluting Stent Implantation | ICR Journal.” https://www.icrjournal.com/articles/dual-antiplatelet-therapy-after-drug-eluting-stent-implantation (accessed Jun. 28, 2022).

[43] J. W. Eikelboom, J. Hirsh, F. A. Spencer, T. P. Baglin, and J. I. Weitz, “Antiplatelet Drugs: Antithrombotic Therapy and Prevention of Thrombosis, 9th ed: American College of Chest

Physicians Evidence-Based Clinical Practice Guidelines," *CHEST*, vol. 141, no. 2, pp. e89S-e119S, Feb. 2012, doi: 10.1378/chest.11-2293.

[44] E. S. Huang, L. L. Strate, W. W. Ho, S. S. Lee, and A. T. Chan, "Long-Term Use of Aspirin and the Risk of Gastrointestinal Bleeding," *Am. J. Med.*, vol. 124, no. 5, pp. 426–433, May 2011, doi: 10.1016/j.amjmed.2010.12.022.

[45] L. Wallentin *et al.*, "Ticagrelor versus clopidogrel in patients with acute coronary syndromes," *N. Engl. J. Med.*, vol. 361, no. 11, pp. 1045–1057, Sep. 2009, doi: 10.1056/NEJMoa0904327.

[46] "Twelve or 30 Months of Dual Antiplatelet Therapy after Drug-Eluting Stents | NEJM." https://www.nejm.org/doi/10.1056/NEJMoa1409312 (accessed Jun. 28, 2022).

[47] P. Eghtesady *et al.*, "Heparin-Induced Thrombocytopenia Complicating Support by the Berlin Heart," *ASAIO J.*, vol. 51, no. 6, pp. 820–825, Dec. 2005, doi: 10.1097/01.mat.0000185630.83985.49.

[48] "Achieving Totally Local Anticoagulation on Blood Contacting Devices - Gbyli - 2018 - Advanced Materials Interfaces - Wiley Online Library." https://onlinelibrary.wiley.com/doi/10.1002/admi.201700954 (accessed Jun. 28, 2022).

[49] J. L. Harding and M. M. Reynolds, "Combating medical device fouling," *Trends Biotechnol.*, vol. 32, no. 3, pp. 140–146, Mar. 2014, doi: 10.1016/j.tibtech.2013.12.004.

[50] E. J. Falde, S. T. Yohe, Y. L. Colson, and M. W. Grinstaff, "Superhydrophobic materials for biomedical applications," *Biomaterials*, vol. 104, pp. 87–103, Oct. 2016, doi: 10.1016/j.biomaterials.2016.06.050.

[51] P. Zhang and F. Y. Lv, "A review of the recent advances in superhydrophobic surfaces and the emerging energy-related applications," *Energy*, vol. 82, pp. 1068–1087, Mar. 2015, doi: 10.1016/j.energy.2015.01.061.

[52] S. Nagappan and C.-S. Ha, “Emerging trends in superhydrophobic surface based magnetic materials: fabrications and their potential applications,” *J. Mater. Chem. A*, vol. 3, no. 7, pp. 3224–3251, Feb. 2015, doi: 10.1039/C4TA05078A.

[53] D. Helmer *et al.*, “Transparent, abrasion-insensitive superhydrophobic coatings for real-world applications,” *Sci. Rep.*, vol. 7, no. 1, Art. no. 1, Nov. 2017, doi: 10.1038/s41598-017-15287-8.

[54] Y. Y. Yan, N. Gao, and W. Barthlott, “Mimicking natural superhydrophobic surfaces and grasping the wetting process: A review on recent progress in preparing superhydrophobic surfaces,” *Adv. Colloid Interface Sci.*, vol. 169, no. 2, pp. 80–105, Dec. 2011, doi: 10.1016/j.cis.2011.08.005.

[55] Y. Y. Yan, N. Gao, and W. Barthlott, “Mimicking natural superhydrophobic surfaces and grasping the wetting process: A review on recent progress in preparing superhydrophobic surfaces,” *Adv. Colloid Interface Sci.*, vol. 169, no. 2, pp. 80–105, Dec. 2011, doi: 10.1016/j.cis.2011.08.005.

[56] R. N. Wenzel, “RESISTANCE OF SOLID SURFACES TO WETTING BY WATER,” *Ind. Eng. Chem.*, vol. 28, no. 8, pp. 988–994, Aug. 1936, doi: 10.1021/ie50320a024.

[57] A. B. D. Cassie and S. Baxter, “Wettability of porous surfaces,” *Trans. Faraday Soc.*, vol. 40, no. 0, pp. 546–551, Jan. 1944, doi: 10.1039/TF9444000546.

[58] Gh. Barati Darband, M. Aliofkhazraei, S. Khorsand, S. Sokhanvar, and A. Kaboli, “Science and Engineering of Superhydrophobic Surfaces: Review of Corrosion Resistance, Chemical and Mechanical Stability,” *Arab. J. Chem.*, vol. 13, no. 1, pp. 1763–1802, Jan. 2020, doi: 10.1016/j.arabjc.2018.01.013.

[59] A. Marmur, “Wetting on Hydrophobic Rough Surfaces: To Be Heterogeneous or Not To Be?,” *Langmuir*, vol. 19, no. 20, pp. 8343–8348, Sep. 2003, doi: 10.1021/la0344682.

[60] A. K. Kota, G. Kwon, and A. Tuteja, “The design and applications of superomniphobic surfaces,” *NPG Asia Mater.*, vol. 6, no. 7, Art. no. 7, Jul. 2014, doi: 10.1038/am.2014.34.

[61] M. Ma and R. M. Hill, “Superhydrophobic surfaces,” *Curr. Opin. Colloid Interface Sci.*, vol. 11, no. 4, pp. 193–202, Oct. 2006, doi: 10.1016/j.cocis.2006.06.002.

[62] Z. Guo, W. Liu, and B.-L. Su, “Superhydrophobic surfaces: From natural to biomimetic to functional,” *J. Colloid Interface Sci.*, vol. 353, no. 2, pp. 335–355, Jan. 2011, doi: 10.1016/j.jcis.2010.08.047.

[63] “Kelly Chemical Corporation.” http://www.kellychemical.com/en/index_en.php?showPcWeb= (accessed Jun. 28, 2022).

[64] B. Arkles, “and Silane Surface Modification,” p. 84.

[65] “Anti-Icing Superhydrophobic Coatings | Langmuir.” https://pubs.acs.org/doi/10.1021/la902882b (accessed Jun. 28, 2022).

[66] R. J. Daniello, N. E. Waterhouse, and J. P. Rothstein, “Drag reduction in turbulent flows over superhydrophobic surfaces,” *Phys. Fluids*, vol. 21, no. 8, p. 085103, Aug. 2009, doi: 10.1063/1.3207885.

[67] R. Fürstner, W. Barthlott, C. Neinhuis, and P. Walzel, “Wetting and Self-Cleaning Properties of Artificial Superhydrophobic Surfaces,” *Langmuir*, vol. 21, no. 3, pp. 956–961, Feb. 2005, doi: 10.1021/la0401011.

[68] “Hierarchically Structured Superoleophobic Surfaces with Ultralow Contact Angle Hysteresis - Kota - 2012 - Advanced Materials - Wiley Online Library.” https://onlinelibrary.wiley.com/doi/10.1002/adma.201202554 (accessed Jun. 28, 2022).

[69] K. Bartlet, S. Movafaghi, A. Kota, and K. C. Popat, “Superhemophobic titania nanotube array surfaces for blood contacting medical devices,” *RSC Adv.*, vol. 7, no. 56, pp. 35466–35476, Jul. 2017, doi: 10.1039/C7RA03373G.

[70] T. Sun, H. Tan, D. Han, Q. Fu, and L. Jiang, “No Platelet Can Adhere—Largely Improved Blood Compatibility on Nanostructured Superhydrophobic Surfaces,” *Small*, vol. 1, no. 10, pp. 959–963, 2005, doi: https://doi.org/10.1002/smll.200500095.

[71] “Reduced platelet adhesion and improved corrosion resistance of superhydrophobic TiO2-nanotube-coated 316L stainless steel - ScienceDirect.” https://www.sciencedirect.com/science/article/abs/pii/S0927776514006511?via%3Dihub (accessed Jun. 28, 2022).

[72] M. Kulkarni, A. Mazare, P. Schmuki, and A. Iglič, “Biomaterial surface modification of titanium and titanium alloys for medical applications,” 2014. https://www.semanticscholar.org/paper/Biomaterial-surface-modification-of-titanium-and-Kulkarni-Mazare/1f425f822e4af189acca474d4092e28f5a1a20f4 (accessed Jun. 28, 2022).

[73] “Influence of engineered titania nanotubular surfaces on bone cells - ScienceDirect.” https://www.sciencedirect.com/science/article/abs/pii/S0142961207002347?via%3Dihub (accessed Jun. 28, 2022).

[74] B. S. Smith, P. Capellato, S. Kelley, M. Gonzalez-Juarrero, and K. C. Popat, “Reduced in vitro immune response on titania nanotube arrays compared to titanium surface,” *Biomater. Sci.*, vol. 1, no. 3, pp. 322–332, Feb. 2013, doi: 10.1039/C2BM00079B.

[75] “Enhanced hemocompatibility and antibacterial activity on titania nanotubes with tanfloc/heparin polyelectrolyte multilayers - Sabino - 2020 - Journal of Biomedical Materials Research Part A - Wiley Online Library.” https://onlinelibrary.wiley.com/doi/10.1002/jbm.a.36876 (accessed Jun. 28, 2022).

CHAPTER 2

FABRICATION AND CHARACTERIZATION OF TITANIA NANOSTRUCTURED SURFACES

2.1 Introduction

There is a large effect of surface features on the compatibility of medical devices in the body. In recent studies, the compatibility of the surface is increased by modifying the surface features such as topography, chemistry, and wettability. Titanium and its alloys are widely used to make different types of medical devices due to their biocompatibility and favorable mechanical properties. The rough nanostructured feature on titanium surface is produced by modifying the titania oxide layer present on the surface via hydrothermal synthesis for nanoflowers and electrochemical anodization for nanotubes. The superhydrophobic properties such as contact angle above 150° can be obtained when rough surface texture is combined with the low surface-energy silane compound. The fouling by blood on blood-contacting medical devices may be prevented using these properties. In this study, fabricated superhydrophobic nanostructured surfaces were evaluated for their surface wettability → measuring contact angles via goniometry, surface chemistry → XPS analysis, surface morphology → SEM imaging, and surface crystallinity → XRD analysis.

2.2 Materials and Methods

2.2.1 Fabrication of Titania Nanoflower (NF) Surfaces

Titania nanoflower surfaces were fabricated using a hydrothermal process. Commercially pure titanium foil (0.25 mm, 95%, Titanium Joe Inc.) was polished gradually with abrasive sheets (150, 240, 320, 400, 800, 1000, and 1500) and cut into 2 cm X 2 cm square. Ti pieces were

sonicated in acetone for 10 mins. After sonication, the Ti pieces were rinsed twice with DI water and plasma treatment was performed for 10 mins. Ti pieces were placed in the solution which was prepared using 99.92% v/v DI water, and 0.08% v/v hydrofluoric acid (HF). 70 mL of DI water was poured into clean polytetrafluoroethylene (PTFE) container and Ti pieces were added. Later, 56 µL of ~50% HF solution (20mM HF) was added to each container and securely tightened. The PTFE containers were then placed on a hot plate with a set temperature of 300 °C for 8 hours. Finally, the surfaces were taken out of the PTFE containers and rinsed gently with DI water.

2.2.2 Fabrication of Titania Nanotube (NT) Surfaces

Titania nanotubes surfaces were fabricated using an electrochemical anodization process where titanium (Ti) was used as an anode and platinum (Pt) was used as a cathode. Commercially pure titanium foil (0.25 mm, 95%, Titanium Joe Inc.) was polished gradually with abrasive sheets (150, 240, 320, 400, 800, 1000, and 1500) and cut into 2 cm X 2 cm square. The Ti pieces were cleaned as follows: Immersed in acetone for 3 mins → sonicated in acetone for 10 mins → cleaned 3 times with deionized (DI) water → cleaned with micro 90 detergent solution and rinsed with DI water → rinsed with isopropyl alcohol and sonicated for 10 mins → sonicated in DI water for 10 mins and rinsed 3 times → dried in the fume hood. Similarly, platinum (Pt) pieces were cleaned as follows: Immersed in isopropyl alcohol for 3 mins → rinsed 3 times with DI water → immersed in nitric acid for 3 mins → scrubbed both sides using cotton swabs → rinsed 3 times with DI water and isopropyl alcohol → dried in the fume hood.

The solution for anodization was prepared using 95% v/v diethylene glycol (DEG), 3% v/v DI water, and 2% v/v HF acid. The 60 mL of prepared solution was poured into 250 mL high-density polyethylene (HDPE) containers. The anode and cathode were exposed to an electrolyte consisting of 2% v/v fluoride ions supplied from a stock of 50% HF. The individual circuits were constructed with titanium surfaces as the anode while platinum foils as cathode; the circuit was

completed by supplying 55 V for 22 hrs using a power source (BK precision model-1623A DC power supply) [1]. The titania nanotube surfaces (NT) were taken out of the solution after 22 hours and rinsed using DI water, isopropyl alcohol, and DI water, respectively. They were then annealed using an oven at a ramp rate of 15 °C/min and a dwell temperature of 530 °C for 3 hours (Thermolyne model-FA7915).

2.2.3 Modification of Titania Nanostructured Surfaces

Control titanium (Ti) and fabricated nanostructured surfaces (NT and NF) were modified using chemical vapor deposition. The Ti, NF, and NT were covered with a bowl on a hot plate and fluorinated via vapor phase silanization with 150 µL of heptadecafluoro-1,1,2,2-tetrahydrodecyl trichlorosilane (referred to as silane) at 120 °C for 1 hr.

The following notation was used in the manuscript: unmodified titanium surface: Ti, unmodified nanotube: NT, unmodified nanoflowers: NF, and surfaces treated with silane: Ti-S, NF-S, and NT-S.

2.2.4 Statistical analysis

Surface characterizations with SEM were done using at least 3 different surfaces for each surface type at 5 different locations on the surface (n_{min}=15). Surface characterizations with contact angles were done with at least 3 different surfaces for each surfaces type at 3 different locations on the surface (n_{min}=9). Statistical one-way ANOVA and student t-tests were completed for all quantitative results. Results were considered statistically significant with a p-value ≤ 0.05. Analysis was done using Image J and OriginLab software.

2.3 Results and Discussion

2.3.1 Characterization of different surfaces

Titanium nanostructured surfaces were characterized using techniques as follows: surface wettability → contact angle goniometry, surface morphology → SEM, surface chemistry → XPS, surface crystallinity → XRD.

Ramè-Hart goniometer was used to characterize the wettability of different surfaces using DI water. Surface wettability has been shown to influence interactions between surfaces and blood constituents [1], [2]. Contact angle (θ) is dependent on the surface properties such as surface area, topography, energy, polarity due to chemistry, etc. There are three categories in which the wettability of a surface can be characterized: hydrophilic if $\theta < 90°$, hydrophobic if $\theta > 90°$ [1], [3], and superhydrophobic if $\theta > 150°$. Results indicate that Ti, NF, and NT surfaces were hydrophilic upon fabrication. After modification with silane, both nanostructured surfaces (NF and NT) became superhydrophobic (NF-S and NT-S) while Ti became hydrophobic (Ti-S) (**Figure 2.3.1**). The total liquid-solid free energy during interaction of the liquid with the textured surface can be distinguished into two different configurations: Wenzel, and Cassie-Baxter state. The solid-liquid interfacial area is increased in the Wenzel state due to the permeation of liquid into the surface topography. This results in the reduction of the θ between the liquid and surface. Cassie-Baxter state is a metastable state in which the air pockets are created between the liquid and surface topography, thus minimizing the interaction, and leading to a high apparent contact angle. Studies have shown that low surface energy and suitable surface topography can be used to achieve the Cassie-Baxter state.

The results indicate that the Ti surface is hydrophilic which is expected because it is a non-textured surface and has a higher water-solid interfacial surface area (**Figure 2.3.1**). The results indicate that by modification with silane, surfaces become hydrophobic or superhydrophobic. Ti-S became hydrophobic due to the presence of silane on the non-textured Ti surface and have a higher water-solid interfacial surface area due to the Wenzel state. The low

solid surface energy of fluorocarbons in silane helped to reduce the surface contact [4]–[6]. The NF and NT surfaces are hydrophilic due to the higher water-solid interfacial area resulting from the surface topography. In NF-S and NT-S, the texture and chemistry play an important role to make surfaces superhydrophobic along with silane. The lower water-solid interfacial surface areas on NF-S and NT-S surfaces due to the presence of silane and surface topography attributed to higher contact angles ($\theta > 150°$) compared to Ti, Ti-S, NF, and NT surfaces. (**Figure 2.3.1**).

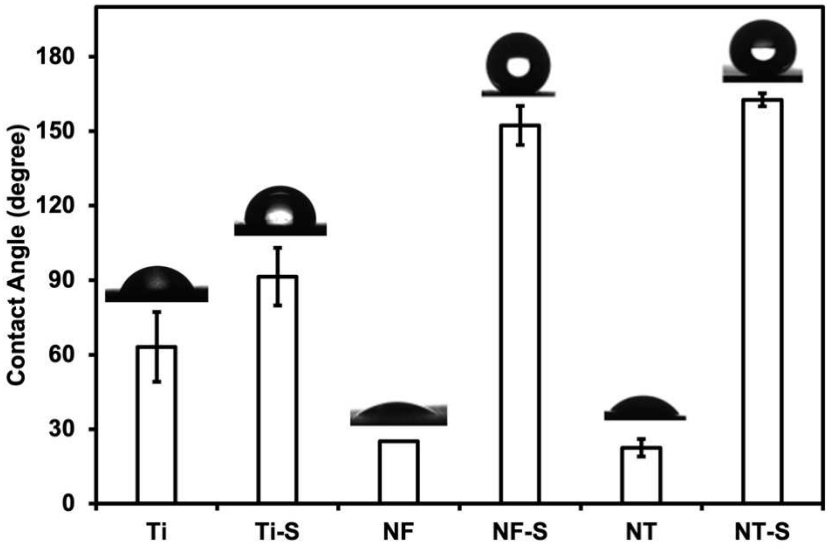

Figure 2.3.1: Static contact angles of DI water (10 µL) droplets on different surfaces. No significant differences in contact angle on NF and NT. Significant differences in contact angles for all other surfaces ($p < 0.05$). Error bars represent standard deviation. Statistical significance is provided in Table 2.

SEM was used to characterize the surface morphology of different surfaces (**Figure 2.3.2**). SEM images of Ti do not show any unique topography. As expected, the morphology of the surface has roughness due to the processing and it is not atomically smooth. SEM images of NF show a uniform petal formation which is a unique texture topography compared to non-textured Ti. The following reaction takes place when the Ti surface is exposed to ~50% HF solution under hydrothermal conditions:

First, Ti reacts with HF to form H_2TiF_6:

$$Ti + 6HF \rightarrow H_2TiF_6 + 2H_2\,(g) \quad (1)$$

More H_2TiF_6 is produced with the continuation of reaction 1. $Ti(OH)_4$ is formed when H_2TiF_6 combines with H_2O:

$$H_2TiF_6 + 4H_2O \rightarrow Ti(OH)_4 + 6HF \quad (2)$$

Under the hydrothermal condition, $Ti(OH)_4$ turns into TiO_2 which nucleates and grows:

$$Ti(OH)_4 \rightarrow TiO_2 + 2H_2O \quad (3)$$

HF further etches the formed TiO_2 due to its corrosive property and the process continues to form nanoflowers on the surface:

$$TiO_2 + 6HF \rightarrow H_2TiF_6 + 2H_2O \quad (4)$$

The NF are crystals that grow out of the surface and assemble in flower formation. This formation occurs due to the oxidation process via hydrothermal treatment in the presence of HF and DI water at 300°C in a controlled environment. The HF etches the Ti surface and forms TiO_2. The continuous dissolution of H_2TiF_6 and deposition of the TiO_2 process results in the formation of nanoflowers on the surface [7].

SEM images of NT shows vertically oriented, immobilized uniform tubes coming out of the surface which is a unique texture topography compared to non-textured Ti. The following reaction takes place when Ti is exposed to DEG, DI water, and HF solution:

$$Ti + 2H_2O - 4e^- \rightarrow TiO_2 + 4H^+ \quad (5)$$

$$TiO_2 + 6F^- + 4H^+ \rightarrow [TiF_6]^{2-} + 2\,H_2O \quad (6)$$

The formation of nanotubes on the non-textured Ti is due to anodic oxidation [8]. Annealing is performed to crystallize the formed amorphous NT arrays at 530°C for 3 hrs [1]. After modification with silane, there was no significant difference between the surface morphology of Ti compared to Ti-S, NF compared to NF-S, and NT compared to NT-S. Further, the diameter of nanotubes was calculated before and after modification with silane, 99.9 ± 10.21 nm (NT) and

101.5 ± 5.03 nm (NT-S), respectively. There is no significant difference in nanotube diameter after surface modification ($p < 0.05$).

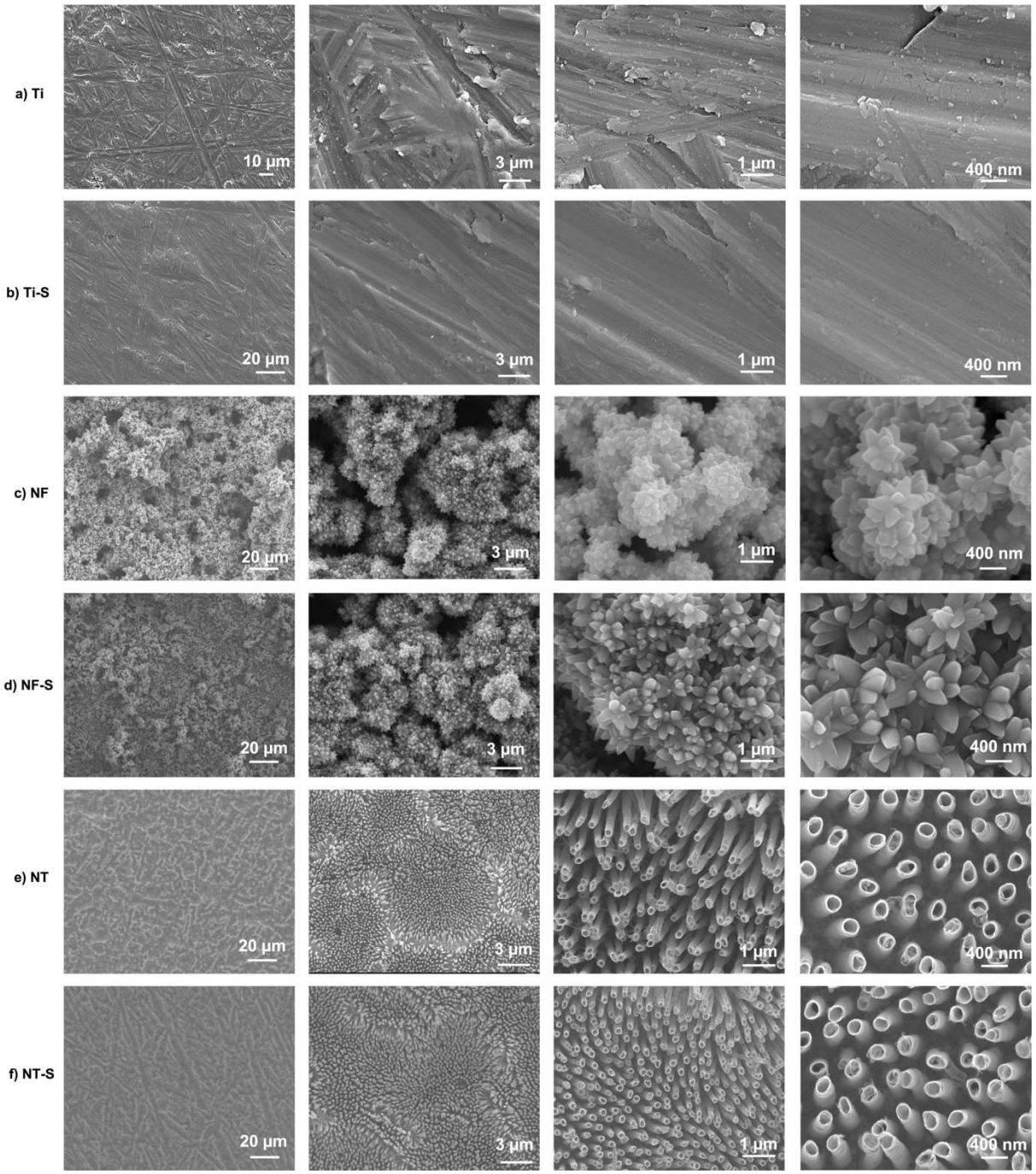

Figure 2.3.2: SEM images of Ti, Ti-S, NF, NF-S, NT, and NT-S at different magnifications (500X, 5,000X, 15,000X, and 30,000X).

XPS was used to characterize the chemistry of different surfaces. It is important to know the surface chemistry (i.e., elemental composition) because it affects cell toxicity, adhesion, interaction with the surface, etc. The silane used to modify the surfaces include fluorine, hence the presence of fluorine in XPS survey spectra indicated successful modification of surfaces. Survey spectra were collected and peaks for Oxygen (O1s), titanium ($Ti2p_{3/2}$), and carbon (C1s) were present in survey spectra for all the surfaces (**Figure 2.3.3**). The survey spectra of Ti showed a small O1s peak and a large C1s peak. The presence of the C1s peak is due to the impurities present on the surface and contamination in the XPS chamber. The survey spectra of Ti-S show a large O1s peak and small C1s peak compared to Ti. This difference is due to the cleaning process which removes the impurities from the surface. There is small fluorine (F1s) peak on Ti-S due to the presence of silane which was used to modify the surface.

Survey spectra of NF show a small C1s peak and large $Ti2p_{3/2}$ peak compared to Ti. The attenuation of the C1s peak is due to the cleaning process and a slightly large $Ti2p_{3/2}$ peak is due to the oxygen plasma treatment [9]. The NF has an F1s peak due to the presence of fluorine from the HF solution (**Equation 1**). The survey spectra of NF-S show a slightly larger C1s peak, and a smaller $Ti2p_{3/2}$ peak compared to NF. This is due to the presence of silane on the surface that leads to attenuation of $Ti2p_{3/2}$ peak after surface modification.

Survey spectra of NT show slightly large O1s and $Ti2p_{3/2}$ peaks compared to Ti which is due to the respective surface reactions (**Equations 5 and 6**). The survey spectra of NT-S show a similar pattern to NT survey spectra but the F1s peak is slightly larger due to the presence of fluorine in the silane which was used to modify the surfaces.

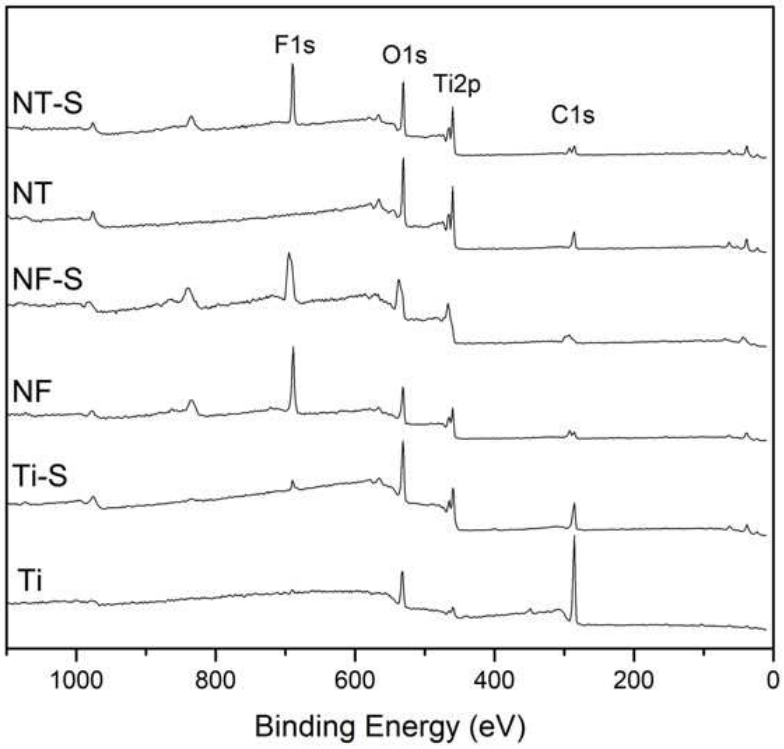

Figure 2.3.3: XPS survey scan of different surfaces. Survey spectra were collected from 0 to 1100 eV with a pass energy of 187.85 eV.

Table 1: XPS elemental composition calculated from survey scans of different surfaces

Elements / Samples	O1s	Ti 2p	C1s	F1s
Ti	17.17	1.78	71.88	0.64
Ti-S	37.74	13.04	37.52	4.91
NF	26.64	8.88	23.56	38.85
NF-S	39.76	12.94	0	43.58
NT	43.80	25.23	28.12	0
NT-S	32.53	11.02	21.70	29.13

XRD was used to characterize the crystallinity of different surfaces (**Figure 2.3.4**). Surface crystallinity plays an important role in wettability and cellular interaction [10], [11]. The different surfaces have anatase, rutile, and titanate phase and XRD helps to determine the presence of these phases. Anatase and rutile phases are metastable minerals of titanium oxide (TiO_2) with a tetragonal structure. Anatase is colorless and the rutile is dark red. Titanate refers to inorganic compounds composed of titanium oxides. The location of intensity peaks of different phases on the graph (**Figure 2.3.4**):

- Intensity peaks at 24° (101) and 62° (204) correspond to the anatase phase (JCPDS no. 21-1272).
- Intensity peaks at 38.1° (002) and 39.9° (101) planes correspond to the metallic Ti phase (JCPDS no. 89-5009).
- Intensity peaks at 76° (110) correspond to the rutile phase of TiO_2 (JCPDS no. 21-1276).
- The intensity peak at 48.7° (030) corresponds to the titanate structure (JCPDS no. 37-951), which suggests the presence of $[TiF_6]^{2-}$.

XRD scan of Ti shows the presence of metallic titanium phase on the surface. XRD scan of Ti-S shows that there is no difference between Ti and Ti-S. XRD scan of NF shows a drastic increase in the intensity of anatase compared to Ti which is due to respective surface reactions (**Equation 5**). The intensity of the metallic titanium phase on the NF surface is attenuated due to the formation of anatase (TiO_2) after oxygen plasma treatment. The oxygen plasma treatment, higher oxidation, and etching during prolonged exposure to HF are responsible for a slight increase in the intensities of titanate and rutile phase on the surface. XRD scan of NF-S shows that there are no drastic differences in the intensities of anatase, rutile, and titanate phases when compared to NF. XRD scan of NT shows a slight increase in the intensities of anatase and rutile phase when compared to Ti due to the respective reaction (**Equation 5**). XRD scan of NT-S shows no differences in the intensities of different phases when compared to NT. The slight

difference in the intensity of the metallic titanium phase (*-Ti) on NT and NT-S surface compared to Ti is due to the respective reaction (**Equation 6**).

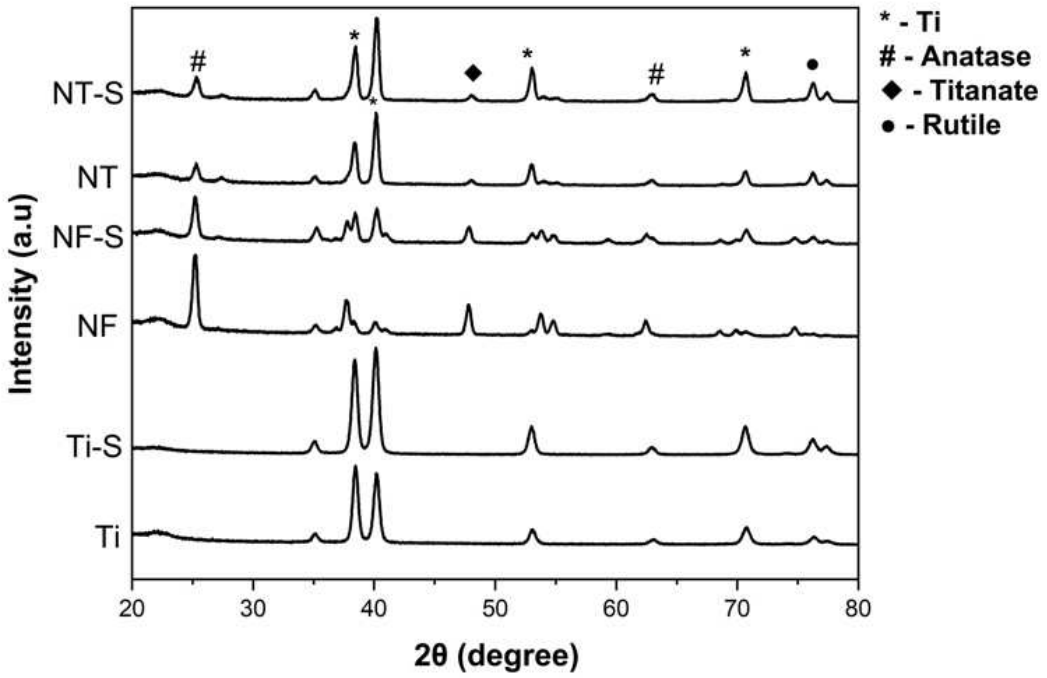

Figure 2.3.4: XRD scans for different surfaces. XRD scans were collected at the 2θ range. Detector scans were run at a step size of 0.01 with a time per step of 1 s.

REFERENCES

[1] B. S. Smith, S. Yoriya, L. Grissom, C. A. Grimes, and K. C. Popat, “Hemocompatibility of titania nanotube arrays,” *J. Biomed. Mater. Res. A*, vol. 95A, no. 2, pp. 350–360, 2010, doi: https://doi.org/10.1002/jbm.a.32853.

[2] J. L. Brash, “Exploiting the current paradigm of blood-material interactions for the rational design of blood-compatible materials,” *J. Biomater. Sci. Polym. Ed.*, vol. 11, no. 11, pp. 1135–1146, 2000, doi: 10.1163/156856200744237.

[3] “Surface Modification of Nanoporous Alumina Surfaces with Poly(ethylene glycol) | Langmuir.” https://pubs.acs.org/doi/10.1021/la049075x (accessed Apr. 29, 2021).

[4] J.-C. Lin, S.-L. Tiong, and C.-Y. Chen, “Surface characterization and platelet adhesion studies on fluorocarbons prepared by plasma-induced graft polymerization,” *J. Biomater. Sci. Polym. Ed.*, vol. 11, no. 7, pp. 701–714, Jan. 2000, doi: 10.1163/156856200743968.

[5] “Biomimetic Fluorocarbon Surfactant Polymers Reduce Platelet Adhesion on PTFE/ePTFE Surfaces: Journal of Biomaterials Science, Polymer Edition: Vol 20, No 5-6.” https://www.tandfonline.com/doi/abs/10.1163/156856209X426439 (accessed May 26, 2022).

[6] “Fluorinated surface-modifying macromolecules: Modulating adhesive protein and platelet interactions on a polyether-urethane - Jahangir - 2002 - Journal of Biomedical Materials Research - Wiley Online Library.” https://onlinelibrary.wiley.com/doi/full/10.1002/jbm.10033?casa_token=wOBXuiSnaLcAAAAA%3Av1M0rCHanv1gHB5dYd6qUgqLYe5YrEob6LIK06kQ5YMkeIBs8Vyv2OJ6f_dWxNEjL_6Q8EJPujxXTZ4 (accessed May 26, 2022).

[7] G. Wu, J. Wang, D. F. Thomas, and A. Chen, “Synthesis of F-Doped Flower-like TiO2 Nanostructures with High Photoelectrochemical Activity,” *Langmuir*, vol. 24, no. 7, pp. 3503–3509, Apr. 2008, doi: 10.1021/la703098g.

[8] G. K. Mor, O. K. Varghese, M. Paulose, N. Mukherjee, and C. A. Grimes, “Fabrication of tapered, conical-shaped titania nanotubes,” *J. Mater. Res.*, vol. 18, no. 11, pp. 2588–2593, Nov. 2003, doi: 10.1557/JMR.2003.0362.

[9] B. Bharti, S. Kumar, H.-N. Lee, and R. Kumar, “Formation of oxygen vacancies and Ti3+ state in TiO2 thin film and enhanced optical properties by air plasma treatment,” *Sci. Rep.*, vol. 6, p. 32355, Aug. 2016, doi: 10.1038/srep32355.

[10] N. Goonoo *et al.*, “Poly(ester-ether)s: III. assessment of cell behaviour on nanofibrous scaffolds of PCL, PLLA and PDX blended with amorphous PMeDX,” *J. Mater. Chem. B*, vol. 3, no. 4, pp. 673–687, 2015, doi: 10.1039/C4TB01350F.

[11] M. M. Shirolkar, D. Phase, V. Sathe, J. Rodríguez-Carvajal, R. J. Choudhary, and S. K. Kulkarni, “Relation between crystallinity and chemical nature of surface on wettability: A study on pulsed laser deposited TiO2 thin films,” *J. Appl. Phys.*, vol. 109, no. 12, p. 123512, Jun. 2011, doi: 10.1063/1.3594695.

CHAPTER 3

HEMOCOMPATIBILITY OF TITANIA NANOSTRUCTURED SURFACES

3.1 Introduction

Thrombosis may occur on the biomedical devices when they come in contact with blood and cause life threatening blood clots. Superhydrophobic nanostructured surfaces offer a material-based solution to thrombosis on these devices. The contact angles greater than 150° produced by superhydrophobic surfaces may significantly reduce the contact between blood components and device's surface. In prior research, improved hemocompatibility of the nanostructured surfaces is observed as there was reduction in platelet and leukocyte adhesion and activation on superhydrophobic nanostructured surfaces [1], [2]. This proves that there is limited adsorption of blood plasma protein on the surfaces. In this work, superhydrophobic nanostructured surfaces were characterized by cytotoxicity, erythrocyte adhesion, and cell morphology. The hemocompatibility of the surfaces was determined using different assay such as hemolysis assay → hemolytic activity, thrombin generation assay → thrombin generation, and complement convertase assay → complement activity. The percentage change in cells was also calculated.

3.2 Material and Methods

3.2.1 Cytotoxicity of different surfaces

Cytotoxicity of different surfaces was characterized using lactase dehydrogenase (LDH) assay. After 1.5 hours of incubation with erythrocytes, Erythrocytes suspension (50 µL) was exposed to surfaces and LDH reaction solution (50 µL) was added to each well of a 96 well plate.

The well plate was incubated at 37 °C and 5% CO_2 for 30 mins. The plate reader was used to measure the absorbance of the resulting solution at 490 nm wavelength. Negative control (maximum LDH release) was prepared by lysing erythrocytes using 10% Triton-X100. The positive control was prepared with erythrocyte suspension without any exposure to surfaces. The protocol provided by the manufacturer was followed and cell toxicity was calculated.

3.2.2 Erythrocyte adhesion on different surfaces

Erythrocyte adhesion on different surfaces was characterized using fluorescence microscopy. The Calcein-AM (Invitrogen) was used to stain the live cells on the surfaces. In most eukaryotic cells, the cell viability can be determined using Calcein-AM which is a cell-permeant dye. In live cells, the nonfluorescent Calcein-AM is converted to a green, fluorescent Calcein-AM after acetoxymethyl ester hydrolysis by intracellular esterases.

The Calcein-AM solution was thawed and mixed with 50 µL of dimethyl sulfoxide (DMSO) for each vial to reconstitute the crystal and make a stock solution. 100 µL of stock solution was added to 18 mL of PBS to prepare the staining solution. The erythrocyte suspension (300 µL) from the incubated surfaces was aspirated to remove floating cells and the surfaces were rinsed twice with PBS. The adhered cells on the surfaces were exposed to the staining solution (300 µL) and incubated at room temperature for 20 mins. The staining solution was aspirated, and surfaces were rinsed with 300 µL of PBS. The surfaces were hydrated by adding 300 µL of PBS. The imaging of the surfaces was performed using a FITC MF101 Green filter with a fluorescent microscope (Zeiss). Surfaces were imaged at three different locations and three different magnifications (10X, 20x, and 50x). The images were processed using Image J to calculate the percentage area covered (10x magnification) by the live cells.

3.2.3 Erythrocyte morphology on different surfaces

The morphology of adhered erythrocytes on different surfaces was characterized using SEM. Prior to SEM imaging, the erythrocytes adhered to the surfaces were fixed using a standard fixing procedure. In brief, a fixative solution was prepared using 3% glutaraldehyde, 0.1 M sodium cacodylate, and 0.1 M Sucrose in DI water. The buffer solution was prepared using 0.1 M sodium cacodylate, and 0.1 M Sucrose in DI water. The fixative solution was added to a glass petri dish and surfaces were exposed for 40 mins. Afterward, surfaces were transferred to the buffer solution for 10 mins. The surfaces were dehydrated using different concentrations of ethanol 35%, 50%, 70%, and 100% for 10 mins each. Later, surfaces were exposed to Hexamethyldisilazane (HMDS) for 10 mins to complete the fixation process. The surfaces with fixed erythrocytes were coated with 5 nm of gold to minimize sample charging and imaged at 15 kV. The SEM images of the surfaces were taken at different magnifications (1,000X, 2,500X, and 3,500X).

3.2.4 Thrombin generation on different surfaces

Thrombin generation on different surfaces was characterized using a commercially available thrombin generation assay (HaemoScan) which conforms with the international standard ISO 10993/Part 4 and ASTM F756-08 standards. The manufacturer-provided plasma was exposed to sterilized nanostructured surfaces and manufacturer-provided control surfaces (low-density polyethylene and medical steel, provided with the assay) for 15 mins at 37 °C. The maximum thrombin generation over a period on the surfaces was determined using the manufacturer-provided protocol. Over 4 mins, an average thrombin generation was determined from the solution incubated with different surfaces. The plate reader was used to measure the absorbance of the resulting solution at 405 and 540 nm wavelengths. Thrombin concentration and velocity of thrombin generation were calculated for all the surfaces.

3.2.5 Hemolysis of erythrocytes on different surfaces

Hemolysis of erythrocytes on different surfaces was characterized using a commercially available hemolysis assay kit (HaemoScan) which conforms with the international standard ISO 10993/Part 4 and ASTM F756-08 standards. A total hemoglobin concentration was prepared by adding 10 µL of erythrocyte suspension to 990 µL of lysis fluid provided with the assay. The prepared solution was exposed to sterilized nanostructured surfaces and control surfaces (Buna-S and silicon elastomer, provided with the assay) which were incubated for 24 hours on a horizontal shaker (100 rpm) at 37°C and 5% CO_2. The hemolytic activity on different surfaces was determined by following the protocol provided by the manufacturer. The plate reader was used to measure the absorbance (optical density) of the resulting solution at 415, 450, and 380 nm wavelengths.

3.2.6 Complement convertase activity on different surfaces

Complement convertase activity on different surfaces was characterized using a commercially available complement convertase kit (HaemoScan) which conforms with the international standard ISO 10993/Part 4 and ASTM F756-08 standards. The plasma provided by the manufacturer was used to incubate sterilized nanostructured surfaces and control surfaces (medical steel, polydimethylsiloxane, and low-density polyethylene, provided with the assay) for 24 hours at 37 °C and 5% CO_2. The complement generation on different surfaces was determined by following the protocol provided by the manufacturer. The plate reader was used to measure the absorbance of the resulting solution at a 405 nm wavelength.

3.3 Results and Discussion

3.3.1 Cytotoxicity of different surfaces

Cytotoxicity was characterized using a commercially available LDH assay. The surface chemistry and topography were modified using electrochemical anodization and hydrothermal treatment. So, it is crucial to analyze whether the surface modifications induce any kind of toxicity to the cells. This is essential to analyze if the host body can tolerate the implant made from these surfaces. The LDH assay protocol is based on an enzymatic coupling reaction. Lactate dehydrogenase (LDH) is a cytosolic enzyme present in many different cell types that is released into the cell culture medium upon damage to the plasma membrane. The released LDH from the cells oxidizes lactate which generates NADH. The NADH is used by the diaphorase (flavin-bound enzyme) to reduce a tetrazolium salt (INT) to a red formazan product that can be measured at 490 nm. The level of formazan formation is directly proportional to the amount of LDH released into the medium. The LDH activity of different surfaces was analyzed (**Figure 3.3.1**). The highest LDH activity was in the negative control (C-) as the cells were intentionally lysed to release the maximum possible LDH. The positive control (C+) was prepared by adding erythrocyte suspension to the empty wells in the plate and natural cell death was caused due to the reaction with polystyrene (the material used to make the well plate). The C+ had the lower LDH activity as compared to the C-. Further, there was no significant difference between LDH activity on different surfaces and C+ compared to C-, indicating that electrochemical anodization and hydrothermal treatment of surfaces do not cause any cytotoxic effects on the cells.

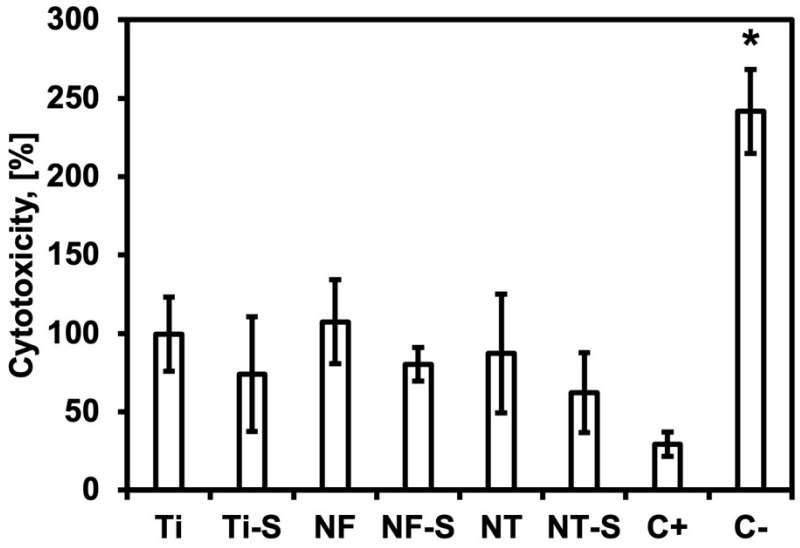

Figure 3.3.1: Cell cytotoxicity for erythrocytes exposed to different surfaces measured using LDH assay. The result indicates no significant differences in the LDH activity on all the surfaces and positive control (100% live cells), whereas the LDH activity for the negative control (100% dead cells) was significantly different than all other surfaces (* → $p < 0.05$). The error bars represent the standard deviation.

3.3.2 Erythrocyte adhesion

Erythrocyte adhesion on different surfaces was characterized using fluorescence microscopy **(Figure 3.3.2.1**). Live cell adhesion on different surfaces was assessed after incubation with erythrocyte suspension for 1.5 hrs and 6 hrs. Cell adhesion was quantified by calculating the area percentage covered by the live cells on the surface using Image J (**Figure 3.3.2.2, Table 2 columns b and c**). The results indicate that there is uniform cell adhesion on Ti after 1.5 hrs and 6 hrs (**Figure 3.3.2.1a**). However, there is a significant decrease in cell adhesion on NF compared to Ti after 1.5 hrs (**Figure 3.3.2.1b, $p < 0.05$, Table 2 column b**). This is due to the morphology and topography of the surface, the change in surface topography at the nanoscale lowers the cell adhesion by forming the frail Cassie-Baxter state between suspended erythrocytes and NF surface.

However, there is no significant difference after 6 hrs since prolonged exposure of the cell solution with the surface. The transition of the Cassie-Baxter state to the Wenzel state occurs due to constant shaking of the 48-well plate for a prolonged period during incubation. The Wenzel state results in a higher erythrocyte-solid interfacial area which results in increased cell adhesion [22]. The results indicate there is a significant decrease in cell adhesion on NT compared to Ti after 6 hrs (**Figure 3.3.2.1e, $p < 0.05$, Table 2 column c**). This is due to the surface topography and morphology; the nanotexture lowers the cell adhesion by forming the less robust Cassie-Baxter state between suspended erythrocytes and NT. After modification with silane, the results indicate that there is a significant difference when Ti-S is compared to NF-S and NT-S. The effect of lowering surface energy between Ti and Ti-S appeared to reduce overall cell adhesion after 1.5 hrs (**$p < 0.05$, Figure 3.3.2.1b, Table 2 column b**). The cell adhesion on Ti-S is less but not significant compared to Ti after 6 hrs (**Figure 3.3.2.1b and Table 2 columns b and c**). This was expected because the constant shaking during incubation results in the transition of the low robust Cassie-Baxter state to the Wenzel state for the erythrocyte suspension. The Wenzel state results in a higher erythrocyte suspension-solid interfacial area which increases the cell adhesion. However, it is observed that there was a significant decrease in cell adhesion; fewer to no cells adhered to the NF-S and NT-S compared to Ti-S after 1.5 hrs and 6 hrs (**$p < 0.05$**, **Table 2 columns b and c, Figure 3.3.2.1d and 3.3.2.1f**). The results were expected because the stability of the Cassie-Baxter state and lower surface energy increased the superhydrophobicity of surfaces that reduced the cell adhesion due to lower interaction between the cells and surfaces. The cell adhesion on NF-S and NT-S were significantly different from that on NF and NT. NF-S and NT-S were shown to have a significant decrease in cell adhesion compared to NF and NT, respectively (**$p < 0.05$, Table 2 columns b and c, Figure 3.3.2.1d and 3.3.2.1f**). This was expected because the NF-S and NT-S have lower surface energy and robust Cassie-Baxter state due to modification with silane which reduces cell interaction with the surface [3]. This suggests that NF-S and NT-S may reduce the formation of thrombus.

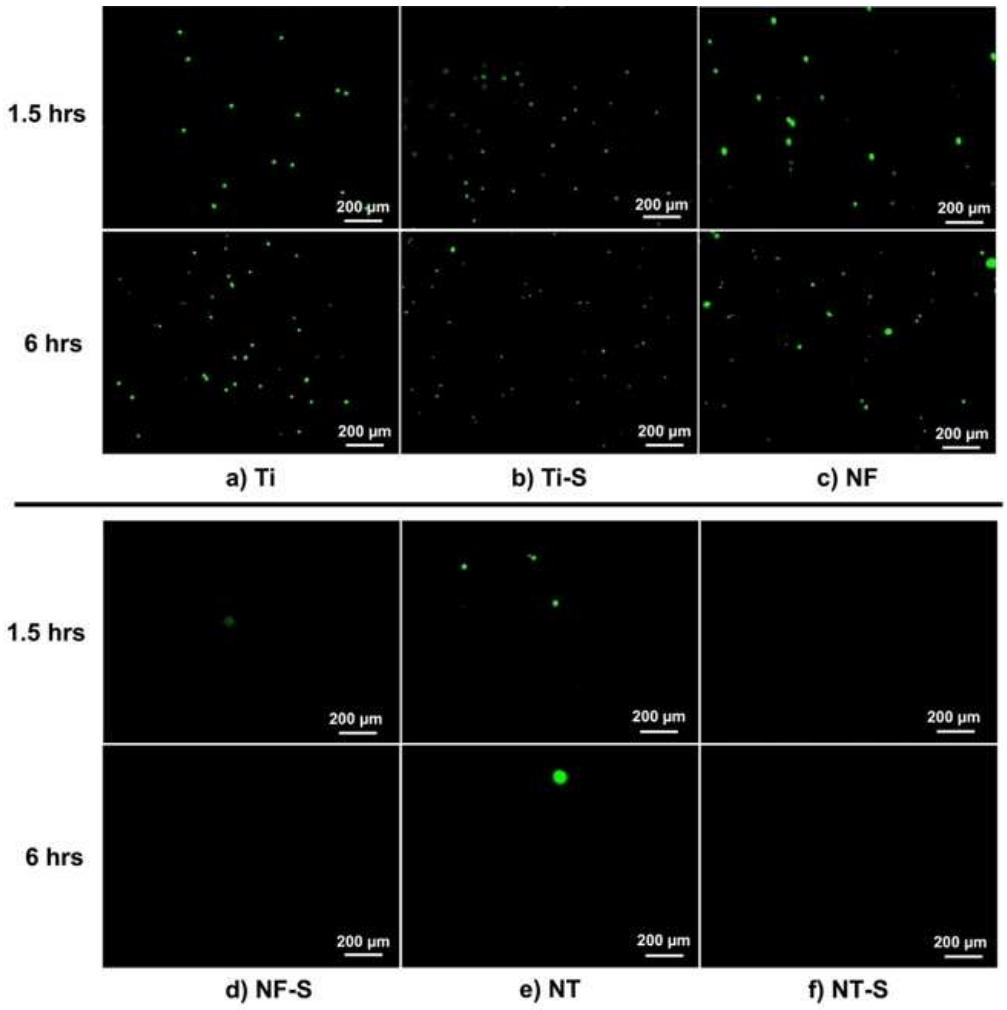

Figure 3.3.2.1: Fluorescence microscopy images of live erythrocyte cells stained with calcein-AM on different surfaces after 1.5 hrs and 6 hrs.

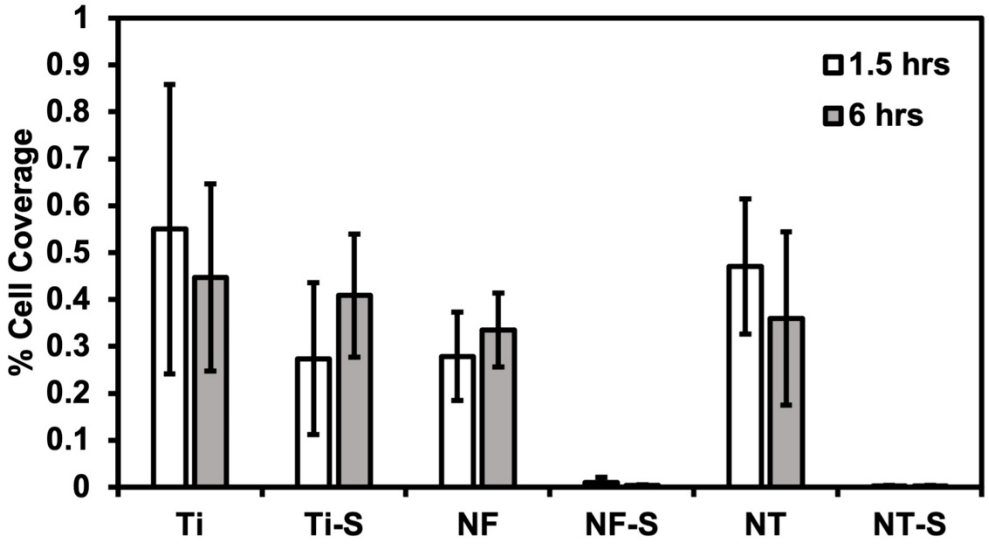

Figure 3.3.2.2: Percentage of live-cell coverage on different surfaces calculated from fluorescence microscopy images. Error bars represent standard deviation. Statistical significance is provided in Table 2.

3.3.3 Cell Morphology

SEM was used to characterize the cell morphology on different surfaces. The surface chemistry and topography influence adhered cell morphology and hence were characterized. Rough surface topography deforms the cellular structure of erythrocytes. Morphological change based on surface chemistry is due to the presence of different phases of titanium dioxide (TiO_2) [5] on different surfaces that interacts with cells (**Figure 2.3.4**). Erythrocytes are small, round, and biconcave (dumbbell-shaped) cells. They contain lipids and proteins, hemoglobin that binds to oxygen, and are anuclear [6]. In general, the erythrocytes with abnormal shapes are known as poikilocytes [7]. Disruptions to the standard biconcave disk morphology of erythrocytes serve as a marker for hemolytic pathologies and oxidative damage to integrated membrane proteins. There are 18 different types of morphological changes experienced by the erythrocytes due to different conditions. In this study, one morphological change, echinocytes (erythrocytes with spicules), was observed. The formation of echinocytes occurs through the process of echinocytosis where the surface area of the outer lipid monolayer increases relative to the inner monolayer. In the body,

this may occur due to pyruvate kinase deficiency, kidney disease, or cancer [7], [8]. Studies have also shown that excess EDTA causes echinocytosis to form echinocytes [8]. However, in this study, since all the cells were exposed to EDTA, the differences in results are due to the surface effects. There are four stages of the cell during the process of echinocytosis [9]:

- Echinocyte 1: A disc with several irregularities on its rim.
- Echinocyte 2: An elliptical body slightly distributed over its surface with different spicules.
- Echinocyte 3: A sphere with evenly spaced sharp spicules. They are about 30–50 in numerous.
- Sphero-Echinocyte: A sphere with shortened and sharpened spicules.

The initial stages (1-3) are partially reversible but the sphero-echinocyte is non-reversible due to extensive membrane loss [10].

The results indicate that the cells adhering to different surfaces experience morphological changes after 6 hrs (**Figure 9**). Sphero-Echinocytes and Stage-3 echinocytes were observed on Ti (**Figure 9a**) due to the presence of TiO_2 (**Figure 4**) [8]. Similar, morphological changes were observed on NF and NT surfaces after 6 hrs (**Figures 9c and 9e**). However, only echinocyte Stage-1 and Stage-2 were observed on the NF and NT surfaces. The results indicate a significant increase in morphological changes in cells on NF compared to Ti (**$p < 0.05$, Table 2 column d**, **Figure 10**) due to the presence of TiO_2 in the form of anatase and titanate phases (**Figure 2.3.4**) and the topography of the surface. The nanoflower topography interacts with the cell membrane similar to how a nanoparticle will interact. Studies have shown that nanoparticles can also cause echinocytosis and related morphological changes in the cells [5]. This increases the outer surface area of the lipid monolayer relative to the inner monolayer. The observed morphological changes in the cells on the NT are higher compared to Ti (**Figure 3.3.3.2**) due to the presence of TiO_2 and the surface topography. The absence of nanoparticles gives NT a smooth topography and provides more surface area compared to Ti. In NT, the trough formed

between tubes and the cavity of the tubes stretches the outer lipid monolayer of the cells which induces morphological change (**Figure 3.3.3.1f**).

After modification with silane, results indicate a significant (**p < 0.05, Table 2 column d**) increase in morphological change that occurs in cells on Ti-S compared to Ti (**Figure 3.3.3.2**). Studies have shown that the surface chemistry of materials (e.g. polymers used for blood collection bags) induces morphological changes in the cells [11]–[13]. Similarly, the presence of silane and surface hydrophobicity induce morphological changes in cells on Ti-S [8]. The erythrocytes were changed to Stage-3 echinocytes and sphero-echinocytes (**Figure 3.3.3.1b**). As expected, silane and roughness of the surface induce morphological change in the cells on NF-S, but it is less compared to NF (**Figure 3.3.3.2**). This is due to the combined effects of surface topography and chemistry which make the NF-S superhydrophobic and decreases cell adhesion (**Figure 3.3.3.1**). The membrane of the cells does not stretch due to the superhydrophobicity that prevents any interaction with the surfaces, and therefore decrease in cell morphology is observed (**Figure 3.3.3.2**). Finally, NT-S showed the least morphological changes compared to other surfaces which were expected due to surface chemistry (presence of silane) and topography (**p < 0.05, Figure 3.3.3.1f, Table 2 column d**). The surface is superhydrophobic due to the robust Cassie-Baxter state further decreasing the cell adhesion compared to NT (**Figure 3.3.3.2**). The superhydrophobicity does not allow cells to adhere and interact with the surface topography, therefore, limiting the contact of cells with the surface and hence no stretching of the cell membrane.

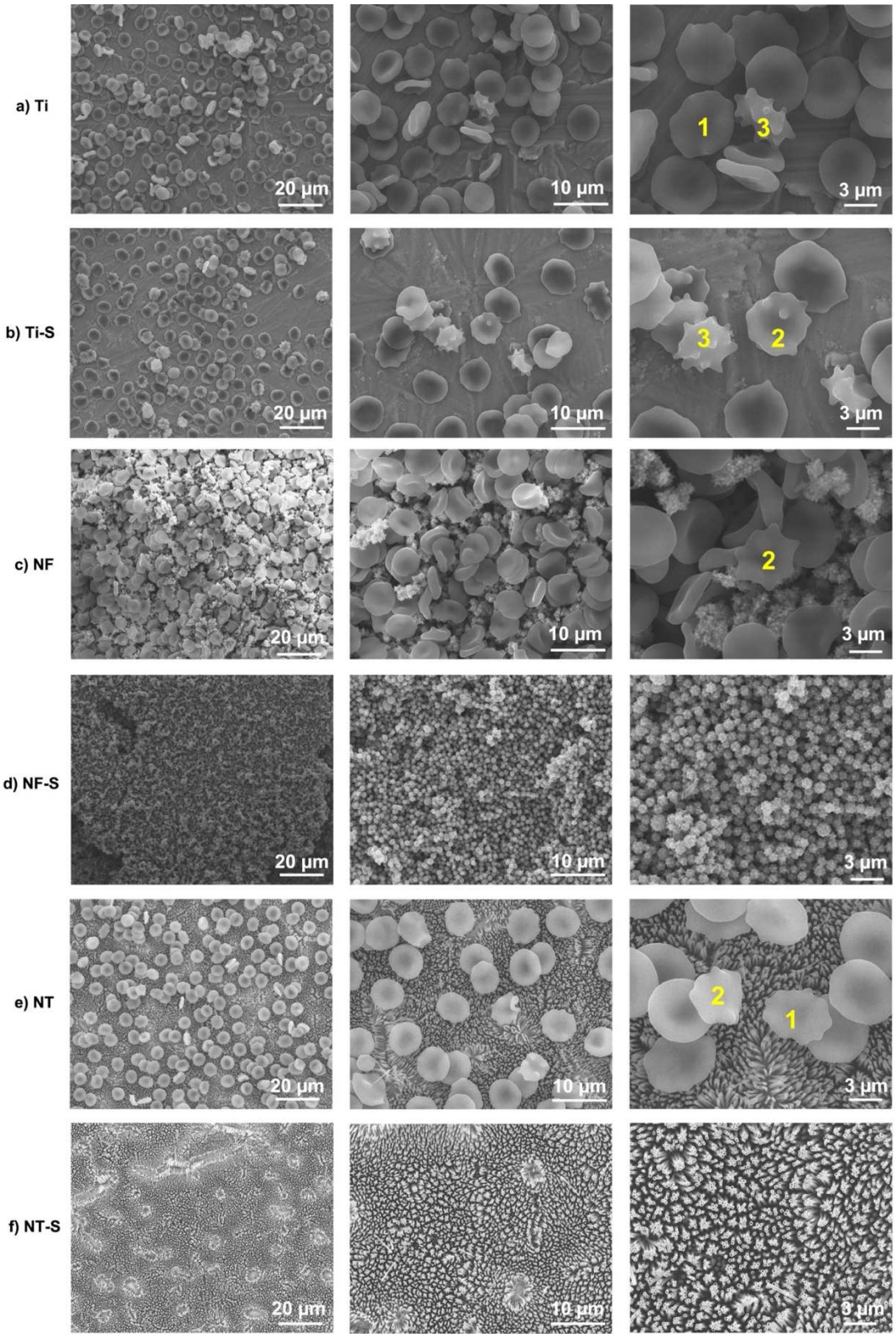

Figure 3.3.3.1: SEM images were taken for Ti, Ti-S, NF, NF-S, NT, and NT-S at different magnifications (1000X, 2500X, and 5,000X) to characterize the morphological changes of the cells. 1, 2, and 3 indicate different stages of echinocytosis.

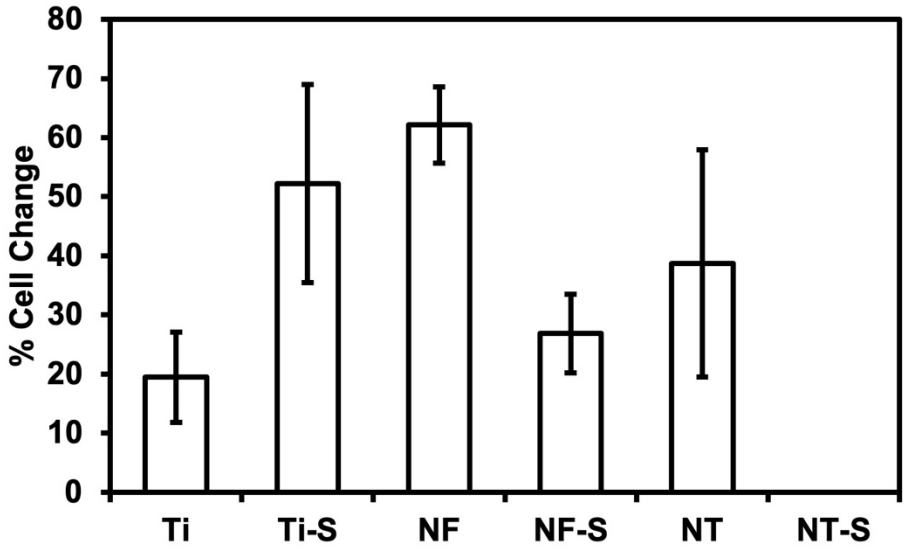

Figure 3.3.3.2: Morphological changes in erythrocytes characterized from SEM images (Figure 3.3.3.1) of different surfaces after 6 hrs of cell adhesion. Error bars represent standard deviation. Statistical significance is provided in Table 2.

3.3.4 Hemolysis

Previous studies have investigated erythrocytes' interaction with different surfaces that result in morphological changes in the cells. However, the presence of a surface may affect cells that have not adhered to the surface but are present in the surrounding environment. Thus, the hemolytic activity on different surfaces was characterized using a commercially available hemolysis assay. The erythrocytes are considered fragile because the membrane of red blood cells experiences dynamic stress when introduced to biomaterials [14]. This results in erythrocyte lysis which can be induced due to surface charge, topography, toxins, metal ions, and chemistry can induce erythrocyte lysis on the implant surface [15]. The release of hemoglobin occurs due to the erythrocyte lysis when cells come in contact with the surface [16], [17]. The amount of hemoglobin released due to erythrocyte lysis can be used as a marker for hemolysis. The results indicate that there were no significant differences in the release of hemoglobin for different surfaces and FDA-approved Buna N (C1) and silicon elastomer (C2) (**Figure 3.3.4.1**).

Hemoglobin plays a vital role in carrying oxygen throughout the body. The results indicate that the hemoglobin is still intact in the non-adhered cells present in the solution and different surfaces do not induce hemolysis.

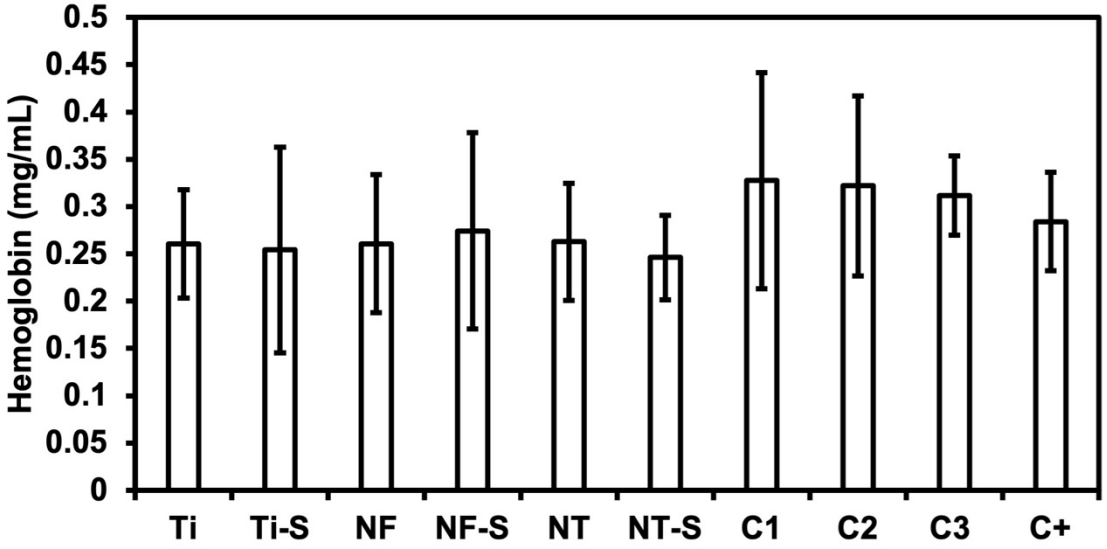

Figure 3.3.4.1: Hemoglobin release from an erythrocyte suspension was measured with a spectrophotometer after an incubation period of 24 h. The C1, C2, C3, and C+ are Buna-N, silicon elastomer, medical steel, and positive control, respectively. There was no significant difference in the release of hemoglobin for different surfaces and FDA-approved Buna N (C1) and silicon elastomer (C2). Error bars represent standard deviations.

3.3.5 Thrombin Generation

The thrombin generation on different surfaces was characterized using a commercially available thrombin generation assay. The coagulation cascade is a complex process that has two definite pathways: intrinsic (contact activation) and extrinsic (tissue factor) pathways which activate the prothrombin to form thrombin [18]. The intrinsic pathway, also known as contact activation, is responsible for thrombin generation on different surfaces. The process initiates when protein Factor XII (coagulation factor) is converted to its activated form FXIIa [19]. The auto-activation of Factor XII occurs when it binds to the surface due to conformational change [20], [21]. The thrombin is formed after several proteins are activated in a chain due to FXII activation

[22]. The thrombin plays a vital role in the conversion of fibrinogen to fibrin. Fibrinogen is primarily responsible for platelet adhesion and plays a vital role in the coagulation cascade [23]. The fibrin forms a mesh-like structure (matrix) through polymerization in which activated platelets and red blood cells get trapped. This leads to the formation of a thrombus on the surface. Moreover, previous studies have shown that erythrocytes were the most efficient cell type in triggering thrombin generation [24]. Therefore, sole adhesion of erythrocytes would not lead to a large amount of thrombus formation because there is no fibrin matrix to trap these erythrocytes. A large amount of thrombin generation is directly proportional to fibrin generation. The inflammatory cell chemotaxis also occurs due to thrombin generation. It is difficult to analyze thrombin's activity due to its half-life. Thrombin generation was measured at different instances by exposing different surfaces and controls (provided by the manufacturer) to plasma provided by the manufacturer. The data was collected over a period of 4 mins, and it was observed that the medical steel (MS) had significantly higher thrombin generation velocity compared to low-density polyethylene (L1), titanium (Ti), and modified nanostructured surfaces (**Figure 3.3.5.1**).

Results indicate that the Ti has thrombin generation which is due to the formation of fibrin mesh and adhesion of erythrocytes on the surface (**Figure 3.3.5.1**). However, there is less thrombin generation on NF compared to Ti (**Figure 3.3.5.1**). Previous studies have shown that there is less platelet activation on NF [25]. However, there is a small amount of thrombin generated on the surface, even though there is less fibrin formation, and more erythrocytes present on the surface. This is due to the effect of surface nanotopography on the cells (**Figure 3.3.5.1**). Previous studies have shown that the damage to the cell membrane exposes more phosphatidylserine (phospholipids) which is important for the assembly of the initial complexes between coagulation factors [8], [24] and the high hydrophilicity nature of the surface resists protein adsorption due to the presence of tightly bound water molecules [26]. This demonstrates that the erythrocytes are important in thrombus formation. The decrease in thrombin generation on NF makes it an ideal surface for blood-contacting medical devices, however, previous results

indicate a greater number of adhered cells undergo morphological change on NF (**Figure 3.3.3.2**). Nevertheless, there is less thrombin generation on NT compared to Ti (**Figure 3.3.5.1**). Previous studies have shown that there is less fibrinogen adsorption on the NT surface indicating a decrease in fibrin formation and thus decreasing thrombin generation [27].

After modification with silane, results indicate that the thrombin generated on Ti-S is similar to Ti (**Figure 12**). Similar to Ti, erythrocytes get trapped in the fibrin matrix resulting in thrombin generation, and also the release of phosphatidylserine (phospholipids) plays a vital role in the formation of the initial coagulation complex. Nevertheless, there is more thrombin generation on NF-S compared to Ti-S (**Figure 3.3.5.1**) because of surface chemistry and topography. Similar to NF, the damage to the cell membrane causes the formation of echinocytes [8], [24]. However, NT-S showed the least thrombin generation compared to Ti-S (**Figure 3.3.5.1**). This was expected due to a decrease in fibrin formation, cell adhesion, and no morphological change on NT-S (**Figure 3.3.2.2**).

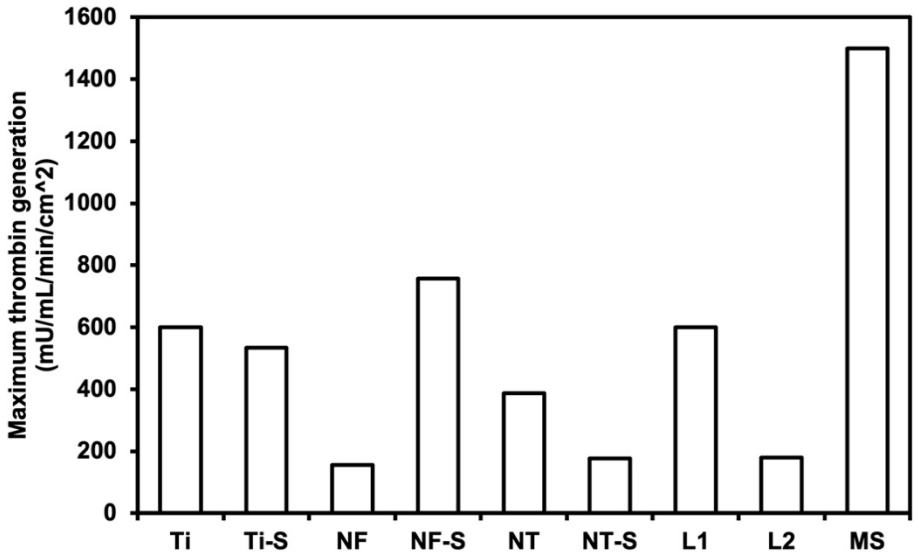

Figure 3.3.5.1: Thrombin generation rate on different surfaces over a period of 4 mins. Results indicate a significant decrease in thrombin generation rate on NF, NT-S, and L2 surfaces compared to medical steel (MS). Error bars represent standard deviation.

3.3.6 Complement activity

The complement activity on different surfaces was characterized using a commercially available complement convertase assay. The natural host defense mechanism of blood by the foreign-body reaction is activated when medical devices encounter blood. The thrombus generation occurs due to the coagulation cascade process (explained in thrombin generation). The intrinsic pathway also includes complement activation which is one of the factors that influences blood clotting. The leukocyte adhesion and activation on the implant surface are assisted by complement activation. The necrosis of normal tissue occurs when adhered leukocytes release lysosomal enzymes and oxygen radicals. The adhered complement factors were measured after different surfaces were incubated with manufacturer-provided plasma. Results indicate that NF and NT had significantly higher complement activation compared to other modified surfaces, medical steel (C1), and low-density polyethylene (C3) surfaces (**Figure 3.3.6.1**).

As expected, Ti had less complement activation due to its biocompatibility and is extensively used for medical implants. However, there was a significant increase in complement activation on NF and NT compared to Ti (**$p < 0.05$, Table 2 column e, Figure 3.3.6.1**). The immune response activation by the body due to the presence of nanostructures on the surfaces leads to a significant increase in complement activation. After modification with silane, there is no significant difference between Ti and Ti-S (**Figure 3.3.6.1**). Previous studies have shown that silane does not affect the immune response. However, there is a significant decrease in complement activation on NF-S and NT-S compared to NF and NT (**$p < 0.05$, Table 2 column e, Figure 3.3.6.1**). This is expected because the superhydrophobicity of the surface does not allow cell adhesion. The lack of adhesion to the surface inhibits immune response activation and thus resulting in a decrease in complement activation.

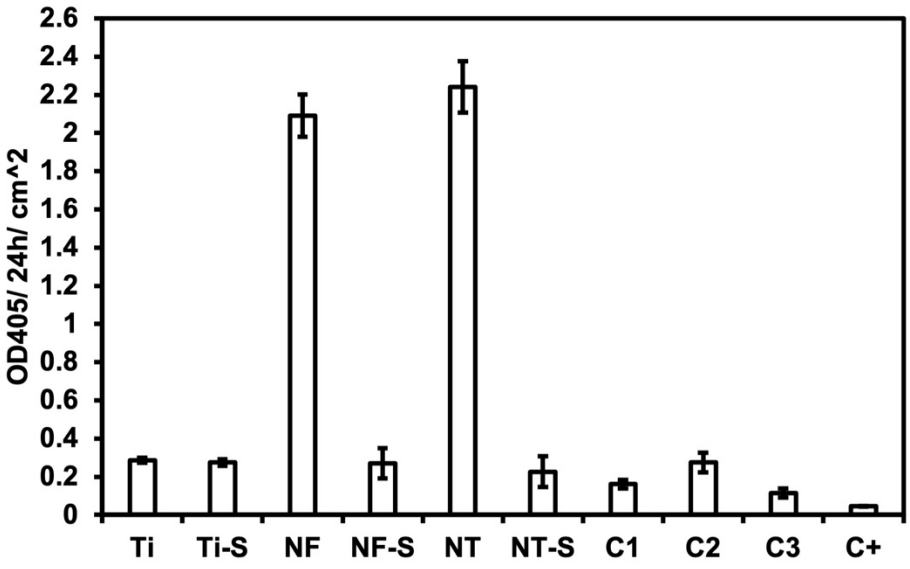

Figure 3.3.6.1: Complement activity on different surfaces after 24 hrs of incubation. Results indicate a significant decrease in complement activity on NF-S and NT-S. Error bars represent standard deviation. Statistical significance is provided in Table 2.

Table 2: Overall statistical comparison of different results based on unmodified and modified surfaces.

Surfaces	(a) Contact Angles	(b) Cell Adhesion (1.5 hrs)	(c) Cell Adhesion (6 hrs)	(d) Erythrocyte morphology	(e) Complement activity
Ti	* * * *	* * *	* * *	* *	* * *
Ti-S	* * *	* * *	* *	* *	* *
NF	* * * *	* * *	* * *	* *	* * *
NF-S	* *	* *	* *	* *	* *
NT	* * *	* * *	* * *	* *	* *
NT-S	*	*	*	*	*

REFERENCES

[1] K. Bartlet, S. Movafaghi, A. Kota, and K. C. Popat, “Superhemophobic titania nanotube array surfaces for blood contacting medical devices,” *RSC Adv.*, vol. 7, no. 56, pp. 35466–35476, Jul. 2017, doi: 10.1039/C7RA03373G.

[2] S. Movafaghi *et al.*, “Hemocompatibility of Superhemophobic Titania Surfaces,” *Adv. Healthc. Mater.*, vol. 6, no. 4, p. 1600717, 2017, doi: 10.1002/adhm.201600717.

[3] “Cassie–Baxter and Wenzel States on a Nanostructured Surface: Phase Diagram, Metastabilities, and Transition Mechanism by Atomistic Free Energy Calculations | Langmuir.” https://pubs.acs.org/doi/full/10.1021/la3018453?casa_token=DFics6d4WhEAAAAA%3Ai_gQ5Yya-89iA8W_1ZBmR27aqbxYqfyxPbFe7oeTkul8oQycrqtbxaBMnBaS438kq2gxUE2Gf29-s6A (accessed Jun. 02, 2022).

[4] D. Murakami, H. Jinnai, and A. Takahara, “Wetting Transition from the Cassie–Baxter State to the Wenzel State on Textured Polymer Surfaces,” *Langmuir*, vol. 30, no. 8, pp. 2061–2067, Mar. 2014, doi: 10.1021/la4049067.

[5] S. M. Tsui *et al.*, “Single red blood cell analysis reveals elevated hemoglobin in poikilocytes,” *J. Biomed. Opt.*, vol. 25, no. 1, p. 015004, Jan. 2020, doi: 10.1117/1.JBO.25.1.015004.

[6] “Shape and Biomechanical Characteristics of Human Red Blood Cells in Health and Disease - PMC.” https://www.ncbi.nlm.nih.gov/pmc/articles/PMC2998922/ (accessed Jun. 02, 2022).

[7] S. S. Bandaru and V. Gupta, “Poikilocytosis,” in *StatPearls*, Treasure Island (FL): StatPearls Publishing, 2022. Accessed: Jun. 02, 2022. [Online]. Available: http://www.ncbi.nlm.nih.gov/books/NBK562141/

[8] “Echinocyte - an overview | ScienceDirect Topics.” https://www.sciencedirect.com/topics/medicine-and-dentistry/echinocyte (accessed Jun. 02, 2022).

[9] G. Lim, “A Numerical Study of Morphologies and Morphological Transformations of Human Erythrocyte based on Membrane Mechanics.,” Dec. 2003, [Online]. Available: https://scholar.google.com/scholar_lookup?&title=A%20Numerical%20Study%20of%20Morphologies%20and%20Morphological%20Transformations%20of%20Human%20Erythrocyte%20based%20on%20Membrane%20Mechanics&publication_year=2003&author=Lim%2CGHW

[10] H. Xia *et al.*, “Washing in hypotonic saline reduces the fraction of irreversibly-damaged cells in stored blood: A proof-of-concept study,” *Blood Transfus. Trasfus. Sangue*, vol. 15, pp. 1–9, May 2017, doi: 10.2450/2017.0013-17.

[11] “Characterization of erythrocyte quality during the refrigerated storage of whole blood containing di-(2-ethylhexyl) phthalate | Blood | American Society of Hematology.” https://ashpublications.org/blood/article/64/6/1270/163850/Characterization-of-erythrocyte-quality-during-the (accessed Jun. 06, 2022).

[12] “An investigation of red blood cell concentrate quality during storage in paediatric-sized polyvinylchloride bags plasticized with alternatives to di-2-ethylhexyl phthalate (DEHP) - Serrano - 2016 - Vox Sanguinis - Wiley Online Library.” https://onlinelibrary.wiley.com/doi/full/10.1111/vox.12355?casa_token=5JzKbQUzXTwAAAA%3A67D9xtvV1q_cC3l2ScNTHcEA-SdsU9n0AlDLX9HEx46hEgG1GZgYlDqpiduHm_bVlz_9B6l62V3etrFH (accessed Jun. 06, 2022).

[13] A. Doctor and P. Spinella, “Effect of Processing and Storage on Red Blood Cell Function In Vivo,” *Semin. Perinatol.*, vol. 36, no. 4, pp. 248–259, Aug. 2012, doi: 10.1053/j.semperi.2012.04.005.

[14] V. Leszczak and K. C. Popat, “Improved in Vitro Blood Compatibility of Polycaprolactone Nanowire Surfaces,” *ACS Appl. Mater. Interfaces*, vol. 6, no. 18, pp. 15913–15924, Sep. 2014, doi: 10.1021/am503508r.

[15] V. K. Manivasagam and K. C. Popat, “In Vitro Investigation of Hemocompatibility of Hydrothermally Treated Titanium and Titanium Alloy Surfaces,” *ACS Omega*, vol. 5, no. 14, pp. 8108–8120, Apr. 2020, doi: 10.1021/acsomega.0c00281.

[16] A. R. Franco *et al.*, “Antimicrobial coating of spider silk to prevent bacterial attachment on silk surgical sutures,” *Acta Biomater.*, vol. 99, pp. 236–246, Nov. 2019, doi: 10.1016/j.actbio.2019.09.004.

[17] K. V. Nemani, K. L. Moodie, J. B. Brennick, A. Su, and B. Gimi, “In vitro and in vivo evaluation of SU-8 biocompatibility,” *Mater. Sci. Eng. C*, vol. 33, no. 7, pp. 4453–4459, Oct. 2013, doi: 10.1016/j.msec.2013.07.001.

[18] V. K. Manivasagam, R. M. Sabino, P. Kantam, and K. C. Popat, “Surface modification strategies to improve titanium hemocompatibility: a comprehensive review,” *Mater. Adv.*, vol. 2, no. 18, pp. 5824–5842, Sep. 2021, doi: 10.1039/D1MA00367D.

[19] L.-C. Xu, J. Bauer, and C. A. Siedlecki, “Proteins, Platelets, and Blood Coagulation at Biomaterial Interfaces,” *Colloids Surf. B Biointerfaces*, vol. 124, pp. 49–68, Dec. 2014, doi: 10.1016/j.colsurfb.2014.09.040.

[20] K. Ekdahl *et al.*, “Contact (kallikrein/kinin) system activation in whole human blood induced by low concentrations of α-Fe 2 O 3 nanoparticles,” *Nanomedicine Nanotechnol. Biol. Med.*, vol. 14, Dec. 2017, doi: 10.1016/j.nano.2017.12.008.

[21] K. Chatterjee, Z. Guo, E. A. Vogler, and C. A. Siedlecki, “Contributions of contact activation pathways of coagulation factor XII in plasma,” *J. Biomed. Mater. Res. A*, vol. 90A, no. 1, pp. 27–34, 2009, doi: 10.1002/jbm.a.32076.

[22] D. Basmadjian, M. V. Sefton, and S. A. Baldwin, “Coagulation on biomaterials in flowing blood: some theoretical considerations,” *Biomaterials*, vol. 18, no. 23, pp. 1511–1522, Dec. 1997, doi: 10.1016/s0142-9612(97)80002-6.

[23] L. A. Wells, H. Guo, A. Emili, and M. V. Sefton, “The profile of adsorbed plasma and serum proteins on methacrylic acid copolymer beads: Effect on complement activation,” *Biomaterials*, vol. 118, pp. 74–83, Feb. 2017, doi: 10.1016/j.biomaterials.2016.11.036.

[24] J. Hong, A. Larsson, K. N. Ekdahl, G. Elgue, R. Larsson, and B. Nilsson, “Contact between a polymer and whole blood: Sequence of events leading to thrombin generation,” *J. Lab. Clin. Med.*, vol. 138, no. 2, pp. 139–145, Aug. 2001, doi: 10.1067/mlc.2001.116486.

[25] Zachary Montgomerie, “SUPERHYDROPHOBIC TITANIA NANOFLOWERS FOR REDUCING ADHESION OF PLATELETS AND BACTERIA,” Colorado State University, 2020.

[26] J. Zheng, L. Li, H.-K. Tsao, Y.-J. Sheng, S. Chen, and S. Jiang, “Strong Repulsive Forces between Protein and Oligo (Ethylene Glycol) Self-Assembled Monolayers: A Molecular Simulation Study,” *Biophys. J.*, vol. 89, no. 1, pp. 158–166, Jul. 2005, doi: 10.1529/biophysj.105.059428.

[27] R. M. Sabino, K. Kauk, S. Movafaghi, A. Kota, and K. C. Popat, “Interaction of Blood Plasma Proteins with Superhemophobic Titania Nanotube Surfaces,” *Nanomedicine Nanotechnol. Biol. Med.*, vol. 21, p. 102046, Oct. 2019, doi: 10.1016/j.nano.2019.102046.

CHAPTER 4

CONCLUSIONS AND FURTURE WORK

4.1 Conclusions

Blood contacting medical devices used today are prone to thrombosis when implanted into the body. First, the blood plasma proteins encounter and get adsorbed onto the surface to initiate thrombosis. This causes adhesion and activation of platelet, and immune response, and eventually leads to blood clotting. The formed clots can obstruct the flow of blood, cause device failure, and can be life-threatening. Device replacement or long-term drug therapies are the current techniques used to solve thrombosis-related issues. Thus, researchers are searching for effective materials-based solutions to these problems. The antiadhesive properties of superhydrophobic materials make them a promising candidate for the prevention of thrombosis. Nonetheless, very few studies have investigated their potential in blood-contacting medical devices. In this study, superhydrophobic titania nanostructured surfaces (NF-S and NT-S) were fabricated and modified for their material properties, biocompatibility, and hemocompatibility.

Titania nanostructured surfaces were fabricated and modified using different techniques. Later, surfaces were evaluated for their properties and characterized for hemocompatibility. The hydrothermal synthesis procedure was performed with Ti-6Al-4V surfaces, an aqueous HF solution, and heat to fabricated nanoflowers (NF). Electrochemical anodization process was used to fabricate nanotubes (NT) on titanium surface in an aqueous solution of diethylene glycol (DEG), HF, and deionized water (DI water). Fluorine-based silane compound was used to modify the fabricated nanostructured surface via vapor-phase deposition. Morphology of the surface was analyzed and revealed insignificant changes between silanized and unsilanized titania

nanostructured surfaces. Surface chemistry analysis revealed changes in fluorine and carbon functional groups on superhydrophobic titania nanostructured surfaces compared to untreated surfaces. The presence of fluorine shows that the surfaces were successfully silanized. Surface crystallinity was conducted and revealed no significant differences in TiO_2 material properties after hydrothermal treatment for NF and electrochemical anodization for NT. It also indicated that modified surfaces were similar to non-modified surfaces with no significant difference. Contact angles were measured to confirm the hydrophilicity, hydrophobicity, and superhydrophobicity of the surfaces. Contact angles (θ) > 150° were observed on modified nanostructured surfaces after silanization making them superhydrophobic.

Following fabrication and modification, the hemocompatibility of titania nanostructured surfaces was analyzed. Cytotoxicity of the surfaces was evaluated using LDH assay after 1.5 hrs of incubation. It was observed that surfaces were non-toxic to the erythrocytes. The thrombin generation assay was used to observe the formation of thrombus on surfaces. It was observed that superhydrophobic nanostructured surfaces do not induce thrombin generation. The hemolysis was analyzed using a hemolysis assay and the results indicate that superhydrophobic nanostructured surfaces do not induce hemolysis. Lastly, complement activity was evaluated on the surfaces and the results indicated that superhydrophobic nanostructured surfaces do not induce complement activity. The silane present on the superhydrophobic nanostructured surfaces does not allow blood and its constituents to adhere thus inhibiting thrombin generation, hemolysis, and complement activation.

In summary, the superhydrophobic nanostructured surfaces decrease the adhesion of blood components. The results indicate that superhydrophobic nanostructured surfaces can provide a stable medical device surface that prevents thrombosis.

4.2 Future Work

In future studies, it would be essential to the observe the effects of variable size of NF and NT on erythrocytes, platelets, proteins, and other blood components. Crucial to observe the effect of change in size on the silane deposition. It would be helpful know the effects of varied silane on the blood components by changing the time. It would be significant to expose the erythrocytes to the surfaces for a prolonged period. All the studies done so far are in static conditions. Cell adhesion and morphological changes on fabricated superhydrophobic nanostructured surfaces should be determined in dynamic conditions. Endothelial cell adhesion and proliferation assays should be used to evaluate endothelialization. Nanostructures are usually fragile and easily damaged. Further studies must examine the ability for these surfaces to remain stable for a longer period. Future research must find methods to make these surfaces more durable.